HHS Public Access

Author manuscript

*Eur J Med Chem*. Author manuscript; available in PMC 2023 May 24.

Published in final edited form as:

*Eur J Med Chem*. 2022 November 05; 241: 114623. doi:10.1016/j.ejmech.2022.114623.

# Identification of 2-hydroxybenzoic acid derivatives as selective SIRT5 inhibitors

**Yanghan Liu**[a,b], **Bikash Debnath**[b], **Surinder Kumar**[c,d], **David B. Lombard**[c,d,*], **Nouri Neamati**[b,**]

[a]State Key Laboratory for Chemistry and Molecular Engineering of Medicinal Resources, Collaborative Innovation Center for Guangxi Ethnic Medicine, School of Chemistry and Pharmaceutical Sciences, Guangxi Normal University, Guilin, 541004, PR China

[b]Department of Medicinal Chemistry, College of Pharmacy and Rogel Cancer Center, University of Michigan, Ann Arbor, MI, 48109, United States

[c]Department of Pathology and Rogel Cancer Center, University of Michigan, Ann Arbor, MI, 48109, United States

[d]Department of Pathology & Laboratory Medicine, Sylvester Comprehensive Cancer Center, Miami, FL, 33136, United States

## Abstract

The sirtuin deacetylase SIRT5 plays important roles in regulating multiple metabolic pathways, and potentially represents an attractive target for the treatment of several human diseases, especially cancer. In this study, we report the identification of the hit compound **11** bearing a 2-hydroxybenzoic acid functional group as a novel SIRT5-selective inhibitor via our medium-throughput thermal shift screening assay. Hit **11** stabilizes SIRT5 in a dose-dependent manner and shows moderate inhibitory activity against SIRT5 and high subtype selectivity over SIRT1, 2, and 3 in a trypsin coupled enzyme-based assay. The carboxylic acid and the adjacent hydroxyl group of **11** are essential for maintaining activity. To further improve the potency of compound **11**, a lead optimization was carried out, resulting in compound **43** with a 10-fold improved potency. Overall, compound **11** represents a promising new chemical scaffold for further investigation to develop SIRT5-selective inhibitors.

### Keywords

SIRT5 inhibitors; Structure-activity relationship; 2-Hydroxybenzoic acid; Molecular docking; Protein-ligand interactions fingerprinting

*Corresponding author. Department of Pathology and Rogel Cancer Center, University of Michigan, Ann Arbor, MI, 48109, United States. dbl68@miami.edu (D.B. Lombard). **Corresponding author. neamati@umich.edu (N. Neamati).

Declaration of competing interest

The authors declare that they have no known competing financial interests or personal relationships that could have appeared to influence the work reported in this paper.

Appendix A. Supplementary data

Supplementary data to this article can be found online at https://doi.org/10.1016/j.ejmech.2022.114623.

## 1. Introduction

Sirtuins are nicotinamide adenine dinucleotide ($NAD^+$) - dependent protein deacylases which are involved in regulating important biological functions, including life span, transcription, DNA repair, protein secretion, and metabolism [1–3]. There are seven sirtuin members encoded in mammalian genomes, SIRT1 to SIRT7, which are distinguished by subcellular localization, biochemical activities, and biological functions [4, 5]. SIRT5, which primarily resides in the mitochondrial matrix, has robust desuccinylation, demalonylation, and deglutarylation activities *in vitro* and *in vivo*, while having very weak deacetylase activity [6–8]. SIRT5 has attracted increasing attention in recent years due to its role in regulating ammonia detoxification, fatty acid oxidation, cellular respiration, ketone body formation, tricarboxylic acid cycle, glycolysis, and reactive oxygen species metabolism [9–16]. Dysregulation of SIRT5 is found in multiple cancers [17–22], such as non-small cell lung cancer, colorectal cancer, breast cancer, hepatocellular carcinoma and melanoma. The development of SIRT5 modulators is likely to be an attractive strategy for the treatment of cancer and metabolic diseases.

To date, only a handful of SIRT5 inhibitors (Fig. 1) have been reported. Among them, some are peptide-based, which generally suffer from limited stability and poor membrane permeability. Several small molecules inhibitors are reported, and many with weak activity and poor selectivity [23–34]. Therefore, the development of novel, potent, and selective SIRT5 inhibitors is highly desirable.

Herein, we report the identification of hit compound **11** (Fig. 2) containing 2-hydroxybenzoic acid functional group as a selective SIRT5 inhibitor using a medium-throughput thermal shift screening. Hit **11** dose-dependently stabilized SIRT5 and showed moderate inhibitory activity against SIRT5 and substantial subtype selectivity over SIRT1, 2, and 3 in a trypsin coupled fluorescence assay. Starting with **11**, a lead optimization guided by molecular docking was conducted that resulted in the identification of compound **43.** Compound **43** has drug-like properties, inhibits SIRT5 in low micromolar range, and is 10 times more potent than the hit **11**.

## 2. Results and discussion

### 2.1. Identification of hit compound 11 as a SIRT5 inhibitor

We developed and optimized a medium throughput thermal shift assay specific for SIRT5 and screened a drug-like library of 5000 inhouse compounds. In this screening campaign, hit compound **11** (Fig. 2A) was identified as a novel SIRT5 inhibitor. Compound **11** stabilized SIRT5 protein with a temperature shift of 1.8 °C (Fig. 2B) in a concentration-dependent manner (Fig. 2C). To further validate above findings, we tested compound **11** in a trypsin coupled fluorescence assay as reported previously [35,36]. As shown in Fig. 2D, compound **11** displayed moderate inhibitory activity against SIRT5 with an $IC_{50}$ of 26.4 ± 0.8 μM. However, **11** showed high selectivity for SIRT5 over SIRT1, 2, and 3 (see Table S1). Even at the highest concentration of 400 μM, no inhibitions against SIRT1–3 were observed.

### 2.2. Structure-activity relationships of analogues of compound 11

To optimize **11** for further studies, we performed molecular docking studies using crystal structure of SIRT5 (PDB ID: 2NYR) [37]. As shown in Fig. 3A, the carboxylate of **11** forms bidentate salt bridge with Arg105 as well as H-bond to Tyr102, in the deep end of the substrate binding pocket. The hydroxyl group forms a H-bond with Val221 and acetyl carbonyl group forms another H-bond with Tyr255. The compound also forms pi-pi interactions with Phe223 and Tyr255.

To assess the effect of the carboxylic acid on the enzymatic inhibitory activities of **11**, compound **12** was tested for its inhibitory activity against SIRT5, in which the carboxylic acid was masked. As shown in Table 1, compound **12** lost nearly all inhibitory activity against SIRT5, confirming the significance of the carboxylic acid group. This result can easily be understood by the docking model (Fig. 3B). Compound **12** does not form a salt bridge and H-bond interactions with key residues, such as Arg105 and Tyr102. To explore the impact of the hydroxyl on efficacy, we synthesized compound **13** in which the hydroxyl group was replaced by a hydrogen atom. Compound **13** is about 8-fold less potent than **11**, highlighting the importance of the hydroxyl group. Although compound **13** forms a salt bridge with Arg105 and pi-pi interactions with Phe223 and Tyr255, it is missing any interactions with Val221, Gly224, and Tyr102. These results validated our model and that the predicted binding mode of **11** with SIRT5 is reasonable and can be used for further optimization.

Having found that the carboxylic acid and the adjacent hydroxyl of **11** are essential for the inhibitory activity against SIRT5, we retained these features and modified the remainder of the molecule. Compounds containing a thiourea group could form stalled intermediates with ADP-ribose in the SIRT5 active sites and effectively inhibit its enzymatic activity. Previously, Olsen's group disclosed the crystal structures of the zebrafish Sirt5 in complex with stalled bicyclic intermediate of an inhibitor containing a thiourea group (PDB ID 6EO0) [30]. Zheng's group reported selective thiourea-based SIRT5 inhibitory warheads [38,39]. Inspired by these studies, we embedded a thiourea functionality into **11** to improve water solubility and SIRT5 inhibitory activity. This strategy led to analogue **14**, with a lower cLogP of 2.74 by comparison with hit **11** (cLogP = 4.04). Analogue **14** is 2 times more potent than **11** against SIRT5 (Table 2). In our molecular docking study, compound **14** binds in a similar fashion to compound **11** (Fig. 4A), forming salt bridge and H-bond interactions with Arg105 and Tyr102. Compound **14** also forms H-bond interactions with Val221 and Tyr255 as well as pi-pi interactions with Phe223 and Tyr255. Accordingly, we selected analogue **14** for further optimization.

To investigate whether modifications on the phenyl group of **14** can improve potency, a series of analogues **15**–**34** with a variety of functional groups at different positions of the benzene ring were designed and synthesized. The biochemical activity results showed that the acetamide group at the *meta*- (**15**) or *ortho*-position (**16**) of the benzene ring decreased the inhibitory activities against SIRT5 compared with analogue **14**, indicating that substitution at *para*-position of the benzene ring is preferred over other positions. A similar trend was observed in other methyl, fluorine, trifluoromethyl or methoxy substituted

derivatives (Table 2). Given the notion that the benzene ring makes pi-pi interactions with Tyr255 in the molecular modeling of compound **14** (Fig. 4A), we assumed that the electron density of the aromatic ring would have a great influence on the interaction intensity between inhibitor and SIRT5. To test the validity of this hypothesis, compounds **17**, **25**, and **20** were synthesized, in which the acetamide was replaced by electron-donating group methyl, methoxy, and electron-withdrawing group fluorine, respectively. Among these three compounds, compound **20** bearing fluoro-substitution is the most potent, indicating that incorporating an electron-withdrawing group on the benzene ring is beneficial for potency enhancement. Replacement of the fluorine with bromine (**31**) or chlorine (**32**) maintained potency in comparison to **20**, suggesting that substituent size may not be a contributing factor. Based on these results, we designed and synthesized compounds **23**, **29**, and **30**, in which the acetamide was replaced by stronger electron-withdrawing group trifluoromethyl, cyano, and nitryl, respectively. As anticipated, compound **30** bearing a nitro substitution at *para*-position of the benzene ring is the most potent, displaying a 6-fold increased potency in comparison with **11**. The molecular docking revealed that carboxylate of compound **30** forms salt bridge with Arg105, and hydroxylate forms H-bond with Val221 (Fig. 4B). Compound **30** also forms a pi-pi interaction with Tyr255. There is also a strong possibility of H-bond interaction between Tyr255 OH group and $NO_2$ group of compound **30** in other docking poses. According to the predicted binding mode of **30** with SIRT5 (Fig. 4B), we speculated that incorporation of additional binding moieties at the *meta*- or *ortho*-position of the benzene ring may improve potency by increasing hydrophobic interactions with surrounding residues. Therefore, a series of di-substituted analogues **35**–**43** were designed and synthesized for further SAR studies. To explore the optimal di-substituted positions, **35** bearing 3,4-difluoropheny substituent and **36** bearing 2,4-difluorophenyl substituent were designed and synthesized. Compound **35** is more potent than **36**, indicating that di-substitution at the 3 and 4 positions of the benzene ring is preferred, which may be due to the steric effects. Therefore, more 3,4 di-substituted compounds (**41**–**43**) were designed and synthesized. As anticipated, **43** was the most potent, showing a 10-fold increased potency in comparison with **11**, in which a nitro substitution and a *N*-benzylsulfamoyl were incorporated at *para*-position and *meta*-position of the benzene ring, respectively. The molecular docking studies (Fig. 4C) indicated that compound **43** docked in a flipped position in such a way that $NO_2$ group forms salt bridge and H-bond with Arg105 and Tyr102. The benzyl amino sulphonyl group is placed in an inner hydrophobic cavity formed by Thr69, Arg71, and Ala59. While the hydroxyl group of compound **43** forms H-bond interaction with Gly224, and the carboxylate forms weak H-bond with Asn226. We plotted the docking scores (GOLD score) vs $pIC_{50}$ values for all compounds (Fig. 5) and observed a highly significant correlation ($R^2 = 0.71$). A protein-ligand interactions fingerprinting was plotted to visualize interactions between key active site residues and all ligands (Fig. 6). All ligands are organized into 5 major clusters. Majority of active compounds ($pIC_{50} > 4.8$) are in clusters 1 and 2 (C1 and C2), moderately active compounds ($4.8 \leq pIC_{50} \geq 4.5$) are in cluster 3 (C3), while inactive compounds ($pIC_{50} < 4.5$) are in clusters 4 and 5 (C4 and C5). The protein-ligand interaction fingerprints plot revealed the importance of residues Arg105, Tyr102, Val221, Phe223, Gly224, and Tyr255 in SIRT5-ligand binding. Salt bridge with Arg105 is critical for this class of compounds to be active. Hydrogen bonds with either Val221, Tyr102, or Gly224 are advantageous for the activity of compounds.

To investigate the selectivity profile, representative compounds **14** and **43** were tested against SIRT1, SIRT2, and SIRT3. We observed that these two compounds displayed no inhibition against these family members even at the highest concentration of 400 μM, showing substantial selectivity for SIRT5 (see Table S1).

### 2.3. Chemistry

Hit compound **11** and its ethylester **12** were prepared according to the procedure shown in Scheme 1. Reaction of 4-amino-2-hydroxybenzoic acid with thiophosgene in hydrochloric acid gave isothiocyanate **46** in 86% yield. Treatment of **46** with ammonium hydroxide afforded thiourea **47**, which was then reacted with **48** to generate compound **11** in 54% yield. Compound **11** was subjected to sulfuric acid in ethanol to give intermediate **49**. Condensation of **49** with acetyl chloride afforded compound **12**.

Synthesis of compound **13** is outlined in Scheme 2. Buchwald coupling of **54** with *tert*-butyl 4-iodobenzoate **55** afforded intermediate **56** *Tert*-butyl deprotection of **56** gave compound **13**.

The synthetic route to compounds **14**–**40** is shown in Scheme 3. The isothiocyanate **46** was reacted with amine **54** to produce compound **14**. Compounds **15**–**40** were prepared by reacting the common intermediate **46** with different amines using the same method as was used for **14**.

Synthesis of compounds **41**–**43** is shown in Scheme 4. Coupling reaction of compound **57a** with benzylthiol afforded the intermediate **58a**. Treatment of **58a** with 1,3-dichloro-5,5-dimethylimidazolidine-2,4-dione **59** gave sulfonyl chloride **60a**. Condensation of **60a** with cyclopentanamine generated the intermediate **62c**. Bromination of **62c** followed by thiazole cyclization reaction afforded the intermediate **65c**. Reacting the intermediate **65c** with **46** afforded compound **41**. Compounds **42** and **43** were obtained using the same procedure as was used for **41**.

## 3. Conclusions

In this study, we designed and optimized a medium throughput thermal shift assay specific for SIRT5 and identified the hit compound **11** as a novel SIRT5 inhibitor. Compound **11** stabilizes SIRT5 in a dose-dependent manner and inhibits SIRT5 enzymatic activity with an $IC_{50}$ value of 26.4 ± 0.8 μM. In a trypsin coupled fluorescence assay, compound **11** was more potent against SIRT5 as compared to SIRT1, SIRT2, and SIRT3. Molecular docking studies indicate that the carboxylate group forms electrostatic interactions and H-bonds with unique residues Arg105 and Tyr102 of SIRT5 in the deep end of substrate binding pocket. The adjacent hydroxyl group of **11** forms a H-bond with Val221. These observations were validated by *in vitro* enzymatic assay, highlighting the necessity of 2-hydroxybenzoic acid moiety for maintaining SIRT5 inhibition. These results indicate that 2-hydroxybenzoic acid could serve as a warhead for the design of selective SIRT5 inhibitors. To improve potency of **11**, a total of 34 new derivatives were designed and synthesized, among which compound **43** is the most potent and displayed a 10-fold increased potency in comparison with hit **11**. In summary, we identified **11** as a promising novel chemical scaffold to target SIRT5 and

indicate that the thermal shift assay is a useful method to discover novel small-molecule SIRT5 inhibitors.

## 4. Experimental section

### 4.1. Chemistry

All reagents and anhydrous solvents were purchased from commercial sources and used without purification, unless specified. Reaction progress was monitored by UV absorbance using thin-layer chromatography (TLC). Flash chromatography was performed using a Biotage Isolera chromatography system equipped with 10 and 25 g Ultra-SNAP Cartridge columns (25 μM spherical silica). $^{1}$H NMR spectra were obtained using a Bruker (300 or 400 MHz) instrument. A Shimadzu LCMS 2020 system was utilized for generating HPLC traces, obtaining mass spectrometry data, and evaluating purity. Purity of final compounds was assessed at 254 nm. Reverse-phase preparative purifications were performed on a Shimadzu LC-20 modular HPLC system. This system utilized a PDA detector and a Kinetex 5 μm XB-C18 100 Å, 150 mm × 21.2 mm column. The purity of all final compounds was >95%.

**2-hydroxy-4-isothiocyanatobenzoic acid (46).—**4-Aminosalicylic acid (3.06 g, 0.02 mol) was suspended in 35 mL of water and 6.7 mL of concentrated hydrochloric acid added and the mixture was stirred at room temperature. To this suspension another 35 mL portion of water was added followed by thiophosgene (2.7 g, 0.024 mol). After 3 h of stirring, the orange color of the thiophosgene was dissipated indicating completion of the reaction. The solid product was filtered; the filter cake was washed multiple times with water and dried over phosphorus pentoxide. This white solid product (3.35 g, 86% yield) was recrystallized from toluene. The pure product was slightly unstable to light. $^{1}$H NMR (400 MHz, DMSO−$d_6$) δ 7.83 (d, $J$ = 8.4 Hz, 1H), 7.00 (d, $J$ = 2.0 Hz, 1H), 6.96 (dd, $J$ = 8.4, 2.1 Hz, 1H).

**2-hydroxy-4-thioureidobenzoic acid (47).—**Compound **46** (3.756 g, 0.019 mol) was dissolved in 70 mL of aqueous ammonia (28%) and the solution stirred overnight. The white solid product (2.98 g, 73% yield) was recrystallized from aqueous ethanol. $^{1}$H NMR (400 MHz, DMSO−$d_6$) δ 11.38 (s, 1H), 9.97 (s, 1H), 8.07 (s, 1H), 7.70 (d, $J$ = 8.7 Hz, 1H), 7.38 (d, $J$ = 2.1 Hz, 1H), 6.96 (dd, $J$ = 8.7, 2.2 Hz, 1H).

**4-((4-(4-acetamidophenyl)thiazol-2-yl)amino)-2-hydroxybenzoic acid (11).—**To a solution of compound **47** (424 mg, 2.0 mmol) in ethanol was added *N*-(4-(2-bromoacetyl)phenyl)acetamide **48** (512 mg, 2.0 mmol). The reaction mixture was refluxed for 3 h. Preparative HPLC purification afforded the pure product **11** as a white solid (400 mg, 54% yield). $^{1}$H NMR (300 MHz, DMSO−$d_6$) δ 10.72 (s, 1H), 10.10 (s, 1H), 7.84 (d, $J$ = 8.5 Hz, 2H), 7.74 (d, $J$ = 8.7 Hz, 1H), 7.67 (d, $J$ = 8.5 Hz, 2H), 7.56 (d, $J$ = 2.1 Hz, 1H), 7.34 (s, 1H), 7.10 (dd, $J$ = 8.9, 2.1 Hz, 1H), 2.07 (s, 3H). $^{13}$C NMR (150 MHz, DMSO−$d_6$) δ 172.3, 168.8, 163.2, 162.5, 150.6, 147.6, 139.4, 131.8, 129.7, 126.6, 119.5, 108.9, 105.9, 103.6, 103.5, 24.5. HRMS (ESI): $m/z$ $[M + H]^+$ calculated for $C_{18}H_{16}N_3O_4S$, 370.0856; found, 370.0860. HPLC purity at 254 nm, 99.5%.

**Ethyl 4-((4-(4-aminophenyl)thiazol-2-yl)amino)-2-hydroxybenzoate (49).—**To a solution of compound **11** (370 mg, 1 mmol) in ethanol (3 mL) was added conc. $H_2SO_4$ (0.2 mL). The reaction mixture was refluxed for 8 h. Preparative HPLC purification afforded the pure product **49** as a white solid (200 mg, 56% yield). $^1$H NMR (400 MHz, DMSO−$d_6$) δ 10.88 (s, 1H), 10.70 (s, 1H), 7.84–7.80 (m, 2H), 7.77 (d, $J$ = 8.8 Hz, 1H), 7.59 (d, $J$ = 2.1 Hz, 1H), 7.30 (s, 1H), 7.12 (dd, $J$ = 8.8, 2.2 Hz, 1H), 7.02 (d, $J$ = 8.5 Hz, 2H), 4.35 (q, $J$ = 7.1 Hz, 2H), 1.35 (t, $J$ = 7.1 Hz, 3H). MS (ESI) 356 $[M + H]^+$.

**Ethyl 4-((4-(4-acetamidophenyl)thiazol-2-yl)amino)-2-hydroxybenzoate (12).—**Compound **49** (30 mg, 0.085 mmol) was dissolved in anhydrous DMF (2 mL). Acetylchloride (10 μL, 0.141 mmol) and DIPEA (40 μL, 0.242 mmol) were added sequentially at 0 °C. The reaction mixture was then allowed to reach ambient temperature and stirred for 2 h. Preparative HPLC purification afforded the pure product **12** as a white solid (29 mg, 86% yield). $^1$H NMR (400 MHz, DMSO−$d_6$) δ 10.87 (s, 1H), 10.71 (s, 1H), 10.06 (s, 1H), 7.86 (d, $J$ = 8.7 Hz, 2H), 7.78 (d, $J$ = 8.8 Hz, 1H), 7.67 (d, $J$ = 8.8 Hz, 2H), 7.57 (d, $J$ = 2.1 Hz, 1H), 7.36 (s, 1H), 7.15 (dd, $J$ = 8.8, 2.2 Hz, 1H), 4.35 (q, $J$ = 7.1 Hz, 2H), 2.07 (s, 3H), 1.35 (t, $J$ = 7.1 Hz, 3H). LCMS (ESI) 398 $[M + H]^+$, 396 $[M - H]^-$. HPLC purity at 254 nm, 99.6%.

**4-((4-(4-acetamidophenyl)thiazol-2-yl)amino)benzoic acid (13).—**To a solution of compound *N*-(4-(2-aminothiazol-4-yl)phenyl) acetamide **54** (233 mg, 1 mmol) in anhydrous DMF (4 mL) was added Pd $(OAc)_2$ (22 mg, 0.1 mmol), BINAP (124 mg, 0.2 mmol), $Cs_2CO_3$ (390 mg, 1.2 mmol) and *tert*-butyl 4-iodobenzoate **55** (234 μL, 1.2 mmol). The resulting mixture was stirred at 100 °C for 16 h. The reaction mixture was then allowed to reach ambient temperature, filtered and concentrated. The crude product was purified by flash column chromatography to provide product **56** (188 mg, 46% yield) as a yellowish solid. The intermediate **56** (41 mg, 0.1 mmol) was dissolved in DCM (2 mL) and TFA (1 mL). After stirring for 2 h, the solvent was evaporated and the residue was purified by HPLC to give the product **13** as a white solid (34 mg, 95% yield). $^1$H NMR (400 MHz, DMSO−$d_6$) δ 10.67 (s, 1H), 10.05 (s, 1H), 7.97–7.92 (m, 2H), 7.90–7.80 (m, 4H), 7.70–7.63 (m, 2H), 7.32 (s, 1H), 2.07 (s, 3H). LCMS (ESI) 354 $[M + H]^+$, 352 $[M - H]^-$. HPLC purity at 254 nm, 99.0%.

**4-(3-(4-(4-acetamidophenyl)thiazol-2-yl)thioureido)-2-hydroxybenzoic acid (14).—**Intermediate **46** (20 mg, 0.1 mmol) and amine **54** (23 mg, 0.1 mmol) were dissolved in anhydrous pyridine (2 mL). The reaction mixture was stirred at 60 °C overnight and then purified by HPLC to isolate the product as a slightly yellow solid (26 mg, 60% yield). $^1$H NMR (400 MHz, DMSO−$d_6$) δ 11.40 (s, 1H), 10.08 (s, 1H), 7.99–7.03 (m, 8H), 2.08 (d, $J$ = 2.4 Hz, 3H). LCMS (ESI) 429 $[M + H]^+$, 427 $[M - H]^-$. HPLC purity at 254 nm, 99.5%.

**4-(3-(4-(3-acetamidophenyl)thiazol-2-yl)thioureido)-2-hydroxybenzoic acid (15).—**Compound **15** was synthesized following the procedure used to prepare compound **14**. $^1$H NMR (400 MHz, DMSO−$d_6$) δ 10.05 (s, 1H), 8.26–7.10 (m, 8H), 2.08 (s, 3H). LCMS (ESI) 429 $[M + H]^+$, 427 $[M - H]^-$. HPLC purity at 254 nm, 99.9%.

**4-(3-(4-(2-acetamidophenyl)thiazol-2-yl)thioureido)-2-hydroxybenzoic acid (16).—**Compound **16** was synthesized following the procedure used to prepare compound **14**. $^1$H NMR (400 MHz, DMSO−$d_6$) δ 13.57 (s, 1H), 12.07 (s, 1H), 11.35 (s, 1H), 8.29–6.87 (m, 8H), 2.16–2.02 (m, 3H). LCMS (ESI) 429 $[M + H]^+$, 427 $[M - H]^-$. HPLC purity at 254 nm, 98.2%.

**2-hydroxy-4-(3-(4-(p-tolyl)thiazol-2-yl)thioureido)benzoic acid (17).—**Compound **17** was synthesized following the procedure used to prepare compound **14**. $^1$H NMR (400 MHz, DMSO−$d_6$) δ 7.81–7.60 (m, 4H), 7.46 (d, $J$ = 2.1 Hz, 1H), 7.29 (t, $J$ = 7.5 Hz, 3H), 2.34 (s, 3H). LCMS (ESI) 386 $[M + H]^+$, 384 $[M - H]^-$. HPLC purity at 254 nm, 99.5%.

**2-hydroxy-4-(3-(4-(m-tolyl)thiazol-2-yl)thioureido)benzoic acid (18).—**Compound **18** was synthesized following the procedure used to prepare compound **14**. $^1$H NMR (400 MHz, DMSO−$d_6$) δ 7.83–7.02 (m, 8H), 2.37 (s, 3H). LCMS (ESI) 386 $[M + H]^+$, 384 $[M - H]^-$. HPLC purity at 254 nm, 99.5%.

**2-hydroxy-4-(3-(4-(o-tolyl)thiazol-2-yl)thioureido)benzoic acid (19).—**Compound **19** was synthesized following the procedure used to prepare compound **14**. $^1$H NMR (400 MHz, DMSO−$d_6$) δ 11.37 (s, 1H), 7.73–7.60 (m, 2H), 7.53–7.45 (m, 1H), 7.40–7.24 (m, 4H), 7.07 (s, 1H), 2.38 (s, 3H). LCMS (ESI) 386 $[M + H]^+$, 384 $[M - H]^-$. HPLC purity at 254 nm, 99.9%.

**4-(3-(4-(4-fluorophenyl)thiazol-2-yl)thioureido)-2-hydroxybenzoic acid (20).—**Compound **20** was synthesized following the procedure used to prepare compound **14**. $^1$H NMR (400 MHz, DMSO−$d_6$) δ 11.41 (s, 1H), 10.80 (s, 1H), 7.93 (ddd, $J$ = 9.1, 5.2, 2.2 Hz, 2H), 7.74 (dd, $J$ = 18.1, 8.6 Hz, 1H), 7.55 (m,2H), 7.42–7.15 (m, 3H). LCMS (ESI) 390 $[M + H]^+$, 388 $[M - H]^-$. HPLC purity at 254 nm, 99.9%.

**4-(3-(4-(3-fluorophenyl)thiazol-2-yl)thioureido)-2-hydroxybenzoic acid (21).—**Compound **21** was synthesized following the procedure used to prepare compound **14**. $^1$H NMR (400 MHz, DMSO−$d_6$) δ 12.02 (s, 1H),δ 11.43 (s, 1H), 10.73 (s, 1H),δ 7.75 (q, $J$ = 11.0, 9.9 Hz, 4H), 7.63–7.42 (m, 2H), 7.21 (d, $J$ = 9.8 Hz, 2H). LCMS (ESI) 390 $[M + H]^+$, 388 $[M - H]^-$. HPLC purity at 254 nm, 99.4%.

**4-(3-(4-(2-fluorophenyl)thiazol-2-yl)thioureido)-2-hydroxybenzoic acid (22).—**Compound **22** was synthesized following the procedure used to prepare compound **14**. $^1$H NMR (400 MHz, DMSO−$d_6$) δ 12.05 (s, 1H),δ 11.41 (s, 1H), 10.89 (s, 1H), 7.99 (s, 1H), 7.75 (dd, $J$ = 17.9, 8.8 Hz, 1H), 7.63 (d, $J$ = 2.1 Hz, 1H), 7.54–7.30 (m, 4H), 7.20 (s, 1H). LCMS (ESI) 390 $[M + H]^+$, 388 $[M - H]^-$. HPLC purity at 254 nm, 99.9%.

**2-hydroxy-4-(3-(4-(4-(trifluoromethyl)phenyl)thiazol-2-yl)thioureido)benzoic acid (23).—**Compound **23** was synthesized following the procedure used to prepare compound **14**. $^1$H NMR (400 MHz, DMSO−$d_6$) δ 12.12 (s, 1H),δ 11.42 (s, 1H), 10.77 (s, 1H),δ 8.12 (d, $J$ = 8.0 Hz, 2H), 7.81 (dd, $J$ = 19.1, 8.4 Hz, 4H), 7.63 (d, $J$ = 2.1 Hz, 1H), 7.19 (s, 1H). LCMS (ESI) 440 $[M + H]^+$, 438 $[M - H]^-$. HPLC purity at 254 nm, 96.4%.

**2-hydroxy-4-(3-(4-(3-(trifluoromethyl)phenyl)thiazol-2-yl)thioureido)benzoic acid (24).—**Compound **24** was synthesized following the procedure used to prepare compound **14**. $^1$H NMR (400 MHz, DMSO−$d_6$) δ 12.12 (s, 1H),δ 11.41 (s, 1H), 10.80 (s, 1H),δ 8.28–8.19 (m, 2H), 7.87–7.69 (m, 4H), 7.63 (d, $J$ = 2.1 Hz, 1H), 7.18 (s, 1H). LCMS (ESI) 440 $[M + H]^+$, 438 $[M - H]^-$. HPLC purity at 254 nm, 98.9%.

**2-hydroxy-4-(3-(4-(4-methoxyphenyl)thiazol-2-yl)thioureido) benzoic acid (25).—**Compound **25** was synthesized following the procedure used to prepare compound **14**. $^1$H NMR (400 MHz, DMSO−$d_6$) δ 11.39 (s, 1H), 7.86–7.71 (m, 3H), 7.63 (s, 1H), 7.33 (s, 2H), 7.04 (dd, $J$ = 8.6, 6.6 Hz, 2H), 3.82 (s, 3H). LCMS (ESI) 402 $[M + H]^+$, 400 $[M - H]^-$. HPLC purity at 254 nm, 99.8%.

**2-hydroxy-4-(3-(4-(3-methoxyphenyl)thiazol-2-yl)thioureido) benzoic acid (26).—**Compound **26** was synthesized following the procedure used to prepare compound **14**. $^1$H NMR (400 MHz, DMSO−$d_6$) δ 11.40 (s, 1H), 10.81 (s, 1H), 7.76 (d, $J$ = 8.7 Hz, 1H), 7.64–7.52 (m, 2H), 7.49–7.35 (m, 3H), 7.28 (s, 1H), 6.99–6.91 (m, 1H), 3.84 (s, 3H). LCMS (ESI) 402 $[M + H]^+$, 400 $[M - H]^-$. HPLC purity at 254 nm, 99.8%.

**2-hydroxy-4-(3-(4-(4-hydroxyphenyl)thiazol-2-yl)thioureido) benzoic acid (27).—**Compound **27** was synthesized following the procedure used to prepare compound **14**. $^1$H NMR (400 MHz, DMSO−$d_6$) δ 11.38 (s, 1H), 9.73 (s, 1H), 7.80–7.56 (m, 4H), 7.50–7.12 (m, 2H), 6.85 (dd, $J$ = 8.6, 6.5 Hz, 2H). LCMS (ESI) 388 $[M + H]^+$, 386 $[M - H]^-$. HPLC purity at 254 nm, 99.9%.

**2-hydroxy-4-(3-(4-(3-hydroxyphenyl)thiazol-2-yl)thioureido) benzoic acid (28).—**Compound **28** was synthesized following the procedure used to prepare compound **14**. $^1$H NMR (400 MHz, DMSO−$d_6$) δ 11.39 (s, 1H), 9.61 (s, 1H), 7.76 (d, $J$ = 8.7 Hz, 1H), 7.63 (d, $J$ = 2.1 Hz, 1H), 7.50–7.37 (m, 1H), 7.35–7.18 (m, 4H), 6.80 (d, $J$ = 7.7 Hz, 1H). LCMS (ESI) 388 $[M + H]^+$, 386 $[M - H]^-$. HPLC purity at 254 nm, 99.5%.

**4-(3-(4-(4-cyanophenyl)thiazol-2-yl)thioureido)-2-hydroxybenzoic acid (29).—**Compound **29** was synthesized following the procedure used to prepare compound **14**. $^1$H NMR (400 MHz, DMSO−$d_6$) δ 12.07 (s, 1H), 11.36 (d, $J$ = 34.0 Hz, 1H), 10.76 (s, 1H), 8.13–8.05 (m, 2H), 7.93 (dd, $J$ = 8.2, 5.5 Hz, 2H), 7.85 (d, $J$ = 6.5 Hz, 1H), 7.79 (d, $J$ = 8.6 Hz, 1H), 7.62 (d, $J$ = 2.1 Hz, 1H), 7.18 (s, 1H). LCMS (ESI) 397 $[M + H]^+$, 395 $[M - H]^-$. HPLC purity at 254 nm, 98.5%.

**2-hydroxy-4-(3-(4-(4-nitrophenyl)thiazol-2-yl)thioureido)benzoic acid (30).—**Compound **30** was synthesized following the procedure used to prepare compound **14**. $^1$H NMR (400 MHz, DMSO−$d_6$) δ 12.12 (s, 1H), 11.41 (s, 1H), 10.75 (s, 1H), 8.39–8.30 (m, 2H), 8.21–8.15 (m, 2H), 7.95 (s, 1H), 7.80 (d, $J$ = 8.6 Hz, 1H), 7.62 (d, $J$ = 2.1 Hz, 1H), 7.17 (s, 1H). LCMS (ESI) 417 $[M + H]^+$, 415 $[M - H]^-$. HPLC purity at 254 nm, 99.2%.

**4-(3-(4-(4-bromophenyl)thiazol-2-yl)thioureido)-2-hydroxybenzoic acid (31).—**Compound **31** was synthesized following the procedure used to prepare compound **14**. $^1$H NMR (400 MHz, DMSO−$d_6$) δ 12.05 (s, 1H), 11.40 (s, 1H), 10.81 (s, 1H), 7.89–7.83 (m,

2H), 7.77 (d, $J$ = 8.7 Hz, 1H), 7.72–7.54 (m, 4H), 7.21 (s, 1H). LCMS (ESI) 450 $[M + H]^+$. HPLC purity at 254 nm, 99.9%.

**4-(3-(4-(4-chlorophenyl)thiazol-2-yl)thioureido)-2-hydroxybenzoic acid (32).—** Compound **32** was synthesized following the procedure used to prepare compound **14**. $^1$H NMR (400 MHz, DMSO−$d_6$) δ 12.03 (s, 1H),δ 11.40 (s, 1H), 10.81 (s, 1H), 7.98–7.88 (m, 2H), 7.77 (d, $J$ = 8.7 Hz, 1H), .69–7.49 (m, 4H), 7.21 (s, 1H). LCMS (ESI) 406 $[M + H]^+$, 404 $[M - H]^-$. HPLC purity at 254 nm, 99.0%.

**2-hydroxy-4-(3-(4-(4-(*N*-methylsulfamoyl)phenyl)thiazol-2-yl) thioureido)benzoic acid (33).—**Compound **33** was synthesized following the procedure used to prepare compound **14**. $^1$H NMR (400 MHz, DMSO−$d_6$) δ 12.06 (s, 1H), 11.41 (s, 1H), 10.79 (s, 1H), 8.11 (d, $J$ = 8.2 Hz, 2H), 7.92–7.72 (m, 4H), 7.63 (d, $J$ = 2.1 Hz, 1H), 7.54–7.05 (m, 2H), 2.45 (dd, $J$ = 5.0, 2.6 Hz, 3H). LCMS (ESI) 465 $[M + H]^+$, 463 $[M - H]^-$. HPLC purity at 254 nm, 98.9%.

**2-hydroxy-4-(3-(4-(3-(*N*-methylsulfamoyl)phenyl)thiazol-2-yl) thioureido)benzoic acid (34).—**Compound **34** was synthesized following the procedure used to prepare compound **14**. $^1$H NMR (400 MHz, DMSO−$d_6$) δ 12.06 (s, 1H), 11.41 (s, 1H), 10.72 (s, 1H), 8.34 (s, 1H), 8.16 (d, $J$ = 7.6 Hz, 1H), 7.87–7.66 (m, 5H), 7.49 (dd, $J$ = 7.4, 3.4 Hz, 1H), 7.16 (d, $J$ = 20.1 Hz, 1H), 2.46 (dd, $J$ = 5.0, 1.7 Hz, 3H). LCMS (ESI) 465 $[M + H]^+$, 463 $[M - H]^-$. HPLC purity at 254 nm, 98.8%.

**4-(3-(4-(3,4-difluorophenyl)thiazol-2-yl)thioureido)-2-hydroxybenzoic acid (35).—**Compound **35** was synthesized following the procedure used to prepare compound **14**. $^1$H NMR (400 MHz, DMSO−$d_6$) δ 12.03 (s, 1H), 11.40 (s, 1H), 10.79 (s, 1H), 7.94 (t, $J$ = 9.9 Hz, 1H), 7.84–7.40 (m, 5H), 7.18 (s, 1H). LCMS (ESI) 408 $[M + H]^+$, 406 $[M - H]^-$. HPLC purity at 254 nm, 99.5%.

**4-(3-(4-(2,4-difluorophenyl)thiazol-2-yl)thioureido)-2-hydroxybenzoic acid (36).—**Compound **36** was synthesized following the procedure used to prepare compound **14**. $^1$H NMR (400 MHz, DMSO−$d_6$) δ 11.39 (s, 1H), 8.02 (s, 1H), 7.75 (dd, $J$ = 19.7, 8.5 Hz, 1H), 7.62 (d, $J$ = 2.1 Hz, 1H), 7.41 (d, $J$ = 13.1 Hz, 2H), 7.20 (d, $J$ = 31.9 Hz, 2H). LCMS (ESI) 408 $[M + H]^+$, 406 $[M - H]^-$. HPLC purity at 254 nm, 99.0%.

**4-(3-(4-(4-cyano-3-fluorophenyl)thiazol-2-yl)thioureido)-2-hydroxybenzoic acid (37).—**Compound **37** was synthesized following the procedure used to prepare compound **14**. $^1$H NMR (400 MHz, DMSO−$d_6$) δ 12.14 (s, 1H), 11.39 (s, 1H), 10.73 (s, 1H), 8.01–7.93 (m, 4H), 7.76 (dd, $J$ = 18.3, 8.6 Hz, 1H), 7.59 (d, $J$ = 2.1 Hz, 1H), 7.20–7.13 (m, 1H). LCMS (ESI) 415 $[M + H]^+$, 413 $[M - H]^-$. HPLC purity at 254 nm, 98.8%.

**4-(3-(4-(4-cyano-2-fluorophenyl)thiazol-2-yl)thioureido)-2-hydroxybenzoic acid (38).—**Compound **38** was synthesized following the procedure used to prepare compound **14**. $^1$H NMR (400 MHz, DMSO−$d_6$) δ 12.08 (s, 1H), 11.40 (s, 1H), 10.77 (s, 1H), 8.19 (q, $J$ = 7.8 Hz, 1H), 8.05–7.94 (m, 1H), 7.87–7.68 (m, 3H), 7.60 (d, $J$ = 2.1 Hz, 1H), 7.15 (d, $J$ = 9.2 Hz, 1H). LCMS (ESI) 415 $[M + H]^+$, 413 $[M - H]^-$. HPLC purity at 254 nm, 99.9%.

**4-(3-(4-(3-fluoro-4-nitrophenyl)thiazol-2-yl)thioureido)-2-hydroxybenzoic acid (39).—**Compound **39** was synthesized following the procedure used to prepare compound **14**. $^1$H NMR (400 MHz, DMSO−$d_6$) δ 12.09 (s, 1H), 11.40 (s, 1H), 10.73 (s, 1H), 8.33–8.22 (m, 1H), 8.14–7.91 (m, 3H), 7.77 (dd, $J$ = 18.4, 8.5 Hz, 1H), 7.60 (d, $J$ = 2.1 Hz, 1H), 7.25–7.03 (m, 1H). LCMS (ESI) 435 $[M + H]^+$, 433 $[M - H]^-$. HPLC purity at 254 nm, 99.9%.

**4-(3-(4-(2-fluoro-4-nitrophenyl)thiazol-2-yl)thioureido)-2-hydroxybenzoic acid (40).—**Compound **40** was synthesized following the procedure used to prepare compound **14**. $^1$H NMR (400 MHz, DMSO−$d_6$) δ 12.15 (s, 1H), 11.41 (s, 0H), 10.74 (s, 1H), 8.40–8.00 (m, 4H), 7.85–7.75 (m, 1H), 7.60 (d, $J$ = 2.1 Hz, 1H), 7.15 (d, $J$ = 9.0 Hz, 1H). LCMS (ESI) 435 $[M + H]^+$, 433 $[M - H]^-$. HPLC purity at 254 nm, 99.8%.

**1-(3-(benzylthio)-4-fluorophenyl)ethan-1-one (58a).—**To a flask were added 1-(3-bromo-4-fluorophenyl)ethan-1-one **57a** (217 mg, 1 mmol), i-$Pr_2$NEt (0.4 mL, 2 mmol) and dry 1,4-dioxane. The mixture was evacuated and backfilled with nitrogen (3 cycles). Catalyst $Pd_2(dba)_3$ (23 mg, 0.025 mmol), Xantphos (29 mg, 0.05 mmol) and the benzylthiol (0.12 mL, 1 mmol) were added and then the mixture was degassed twice more. The mixture was heated under reflux overnight. The reaction mixture was then allowed to reach ambient temperature, filtered and concentrated. The crude product was purified by flash column chromatography to provide pure product **58a** (250 mg, 96% yield) as a yellow solid. $^1$H NMR (400 MHz, Chloroform-$d$) δ 7.90–7.79 (m, 2H), 7.34–7.23 (m, 5H), 7.13 (t, $J$ = 8.7 Hz, 1H), 4.16 (s, 2H), 2.51 (s, 3H). MS (ESI) 261 $[M + H]^+$.

**1-(3-(benzylthio)-4-nitrophenyl)ethan-1-one (58b).—**Compound **58b** was synthesized following the procedure used to prepare compound **58a**. $^1$H NMR (400 MHz, DMSO−$d_6$) δ 8.29 (d, $J$ = 8.5 Hz, 1H), 8.12 (d, $J$ = 1.7 Hz, 1H), 7.86 (dd, $J$ = 8.6, 1.7 Hz, 1H), 7.51–7.44 (m, 2H), 7.40–7.25 (m, 3H), 4.50 (s, 2H), 2.65 (s, 3H). MS (ESI) 288 $[M + H]^+$.

**5-acetyl-*N*-cyclopentyl-2-fluorobenzenesulfonamide (62c).—**To an ice-cold solution of compound 58a (223 mg, 0.858 mmol) in $CH_3CN$-HOAc-$H_2O$ (10 mL-0.6 mL–0.4 mL) was added portion-wise 2,4-dichloro-5,5-dimethylhydantoin (339 mg, 1.72 mmol). The reaction mixture was stirred at 0 °C for 2 h and concentrated to near dryness under vacuum. The crude product was diluted with $CH_2Cl_2$ (16 mL), and the solution cooled down to 0 °C. 5% $NaHCO_3$ aqueous solution (18 mL) was added slowly at 0 °C. The mixture was stirred at 0 °C for 15 min, and the lower organic layer was washed once more with 10% brine solution at < 10 °C. The lower organic layer was dried over $MgSO_4$ and filtered and concentrated to afford the product 60a as a yellow oil, which was used in the next reaction without further purification.

A solution of 5-acetyl-2-fluorobenzenesulfonyl chloride **60a** (78 mg, 0.33 mmol) and cyclopentanamine (39 μL, 0.396 mmol) in dichloromethane was treated with triethylamine (92 μL, 0.66 mmol) and stirred at 0 °C for 2 h. The mixture was purified by flash column chromatography to provide pure product **62c** (75 mg, 80% yield) as a yellow solid. $^1$H NMR (400 MHz, DMSO−$d_6$) δ 8.32–8.26 (m, 2H), 8.16 (d, $J$ = 7.6 Hz, 1H), 7.65–7.56 (m, 1H),

3.50–3.53 (m, 1H), 2.63 (s, 3H), 1.70–1.50 (m, 4H), 1.45–1.28 (m, 4H). MS (ESI) 286 [M + H]$^+$.

**5-acetyl-*N*-benzyl-2-fluorobenzenesulfonamide (62a).—**Compound 62a was synthesized following the procedure used to prepare compound 62c. $^1$H NMR (300 MHz, DMSO−$d_6$) δ 8.70 (t, $J$ = 6.4 Hz, 1H), 8.17 (t, $J$ = 7.2 Hz, 2H), 7.50 (t, $J$ = 9.2 Hz, 1H), 7.20 (d, $J$ = 4.0 Hz, 5H), 4.15 (d, $J$ = 6.2 Hz, 2H), 2.59 (d, $J$ = 1.3 Hz, 3H). MS (ESI) 308 [M + H]$^+$.

**5-acetyl-*N*-benzyl-2-nitrobenzenesulfonamide (62b).—**Compound **62b** was synthesized following the procedure used to prepare compound **62c**. $^1$H NMR (400 MHz, DMSO−$d_6$) δ 8.84 (s, 1H), 8.27 (dd, $J$ = 8.3, 1.8 Hz, 1H), 8.22 (d, $J$ = 1.8 Hz, 1H), 8.07 (d, $J$ = 8.2 Hz, 1H), 7.24–7.12 (m, 5H), 4.19 (s, 2H), 2.61 (s, 3H). MS (ESI) 335 [M + H]$^+$.

**5-(2-aminothiazol-4-yl)-*N*-cyclopentyl-2-fluorobenzenesulfonamide (65c).—**The intermediate **62c** (14.3 mg, 0.05 mmol) was dissolved in acetonitrile (2 mL) followed by addition of tetrabutylammonium-tribromide (25 mg, 0.05 mmol). The reaction mixture was stirred at 60 °C overnight. The solvent was removed; the residue was extracted with dichloromethane and washed with water. The organic layers were combined and concentrated under vacuum to provide the crude product **63c**, which was used in the next step without further purification.

The intermediate **63c** was dissolved in ethanol (2 mL) followed by addition of thiourea (4 mg, 0.05 mmol). The reaction mixture was refluxed for 3 h and then purified by HPLC to isolate the product **65c** as a white solid (11 mg, 62% yield). $^1$H NMR (400 MHz, DMSO−$d_6$) δ 8.24 (dd, $J$ = 7.2, 2.2 Hz, 1H), 8.07 (ddd, $J$ = 8.7, 4.6, 2.3 Hz, 1H), 7.97 (d, $J$ = 7.6 Hz, 1H), 7.45 (dd, $J$ = 10.1, 8.6 Hz, 1H), 7.17 (d, $J$ = 1.7 Hz, 1H), 3.20–3.13 (m, 1H), 1.61–1.52 (m, 4H), 1.36 (tt, $J$ = 12.4, 6.7 Hz, 4H). MS (ESI) 342 [M + H]$^+$.

**5-(2-aminothiazol-4-yl)-*N*-benzyl-2-fluorobenzenesulfonamide (65a).—**Compound **65a** was synthesized following the procedure used to prepare compound **65c**. $^1$H NMR (400 MHz, DMSO−$d_6$) δ 8.51 (t, $J$ = 5.6 Hz, 1H), 8.19 (dt, $J$ = 7.2, 2.2 Hz, 1H), 8.02 (ddd, $J$ = 8.6, 4.7, 2.3 Hz, 1H), 7.37 (t, $J$ = 9.3 Hz, 1H), 7.30–7.16 (m, 5H), 7.13 (d, $J$ = 2.4 Hz, 1H), 4.12 (d, $J$ = 6.3 Hz, 2H). MS (ESI) 364 [M + H]$^+$.

**5-(2-aminothiazol-4-yl)-*N*-benzyl-2-nitrobenzenesulfonamide (65b).—**Compound **65b** was synthesized following the procedure used to prepare compound **65c**. $^1$H NMR (400 MHz, DMSO−$d_6$) δ 8.55 (t, $J$ = 6.2 Hz, 1H), 8.31 (d, $J$ = 1.8 Hz, 1H), 8.13 (dd, $J$ = 8.4, 1.8 Hz, 1H), 7.95 (d, $J$ = 8.4 Hz, 1H), 7.35 (s, 1H), 7.32–7.10 (m, 5H), 4.21 (d, $J$ = 6.2 Hz, 2H). MS (ESI) 391 [M + H]$^+$.

**4-(3-(4-(3-(*N*-cyclopentylsulfamoyl)-4-fluorophenyl)thiazol-2-yl)thioureido)-2-hydroxybenzoic acid (41).—**Intermediate 2-hydroxy-4-isothiocyanatobenzoic acid **46** (20 mg, 0.1 mmol) and amine **65c** (34 mg, 0.1 mmol) were dissolved in anhydrous pyridine (2 mL). The reaction mixture was stirred at 60 °C overnight and then purified by HPLC to isolate the product as a white solid (43 mg, 80%

yield). $^{1}$H NMR (400 MHz, DMSO−$d_6$) δ 12.13 (s, 1H), 11.43 (s, 1H), 10.78 (s, 1H), 8.36 (d, $J$ = 6.8 Hz, 1H), 8.19 (ddd, $J$ = 8.8, 4.6, 2.4 Hz, 1H), 8.03 (t, $J$ = 7.6 Hz, 1H), 7.82–7.65 (m, 3H), 7.61–7.46 (m, 1H), 7.14 (s, 1H), 3.55 (q, $J$ = 7.3 Hz, 1H), 1.69–1.49 (m, 4H), 1.45–1.30 (m, 4H). LCMS (ESI) 537 $[M + H]^+$, 535 $[M - H]^-$. HPLC purity at 254 nm, 99.9%.

**4-(3-(4-(3-(*N*-benzylsulfamoyl)-4-fluorophenyl)thiazol-2-yl)thioureido)-2-hydroxybenzoic acid (42).—**Compound **42** was synthesized following the procedure used to prepare compound **41**. $^{1}$H NMR (400 MHz, DMSO−$d_6$) δ 12.12 (s, 1H), 11.42 (s, 1H), 10.80 (s, 1H), 8.57 (q, $J$ = 6.2 Hz, 1H), 8.28 (s, 1H), 8.13 (s, 1H), 7.82–7.64 (m, 3H), 7.51–7.41 (m, 1H), 7.27–7.03 (m, 6H), 4.15 (d, $J$ = 6.2 Hz, 2H). LCMS (ESI) 559 $[M + H]^+$, 557 $[M - H]^-$. HPLC purity at 254 nm, 99.9%.

**4-(3-(4-(3-(*N*-benzylsulfamoyl)-4-nitrophenyl)thiazol-2-yl)thioureido)-2-hydroxybenzoic acid (43).—**Compound **43** was synthesized following the procedure used to prepare compound **41**. $^{1}$H NMR (400 MHz, DMSO−$d_6$) δ 12.17 (s, 1H), 11.41 (s, 1H), 10.77 (s, 1H), 8.57 (t, $J$ = 6.2 Hz, 1H), 8.36 (d, $J$ = 1.9 Hz, 1H), 8.24 (dd, $J$ = 8.3, 2.0 Hz, 1H), 8.03 (dd, $J$ = 8.3, 4.3 Hz, 1H), 7.88 (s, 1H), 7.81–7.63 (m, 2H), 7.28–7.06 (m, 6H), 4.24 (d, $J$ = 6.2 Hz, 2H). $^{13}$C NMR (125 MHz, DMSO−$d_6$) δ 171.9, 162.1, 146.4, 145.3, 142.9, 140.8, 137.6, 134.7, 131.3, 130.3, 129.8, 128.6, 128.0, 127.6, 127.1, 125.8, 119.2, 118.6, 115.7, 115.6, 113.4, 113.4, 108.9, 46.8. HRMS (ESI): $m/z$ $[M + H]^+$ calculated for $C_{24}H_{20}N_5O_7S_3$, 586.0519; found, 586.0517. HPLC purity at 254 nm, 97.7%.

**Thermal Shift Assay.—**Thermal shift assay was performed using the ThermoFluor instrument from Johnson and Johnson. Briefly, all reactions were carried out in a buffered solution of 20 mM Bis-Tris propane pH = 7.5, 150 mM NaCl at a final concentration of 0.2 mg/ml SIRT5, 0.1 mM 1,8-ANS, and 100 μM compound or DMSO as a vehicle control. The reaction mixtures were prepared in a 384-well microplate with a total volume of 5 μL and then layered with 1.5 μL silicon oil. The plate was sealed with aluminum sealing film and spun at 1000 rpm for 1 min and then heated from 25 °C to 90 °C under continuous ramp heating mode with the ThermoFluor instrument. Each reaction was repeated in quadruplicate. Melt curves were analyzed with the ThermoFluor ++ software.

**Fluorescence-Based Inhibition Assay.—**The inhibition activities of compounds against human SIRT5, SIRT1, SIRT2, and SIRT3 were measured using a fluorescence-based assay as reported [35,36]. For details, see Supporting Information.

**Molecular Docking.—**Compounds were docked onto the active site of SIRT5 (PDB ID: 2NYR) using GOLD (Genetic Optimization for Ligand Docking) software package, version 4.0 (Cambridge Crystallographic Data Centre, Cambridge, U.K.) [40]. Prior to docking, compounds were ionized, energy-minimized, and ten possible conformers were generated with Omega from OpenEye software using the MMFF94S force field [41]. GOLD uses a genetic algorithm to explore the conformational space of a compound inside the binding site of a protein [42,43]. Docking studies were performed using the standard default settings with 100 genetic algorithm (GA) runs on each molecule. For each of the 100 independent GA runs, a maximum of 100,000 operations was performed on a set of five groups with a population of 100 individuals. With respect to ligand flexibility, special care was

taken by including options such as flipping of ring corners, amides, pyramidal nitrogens, secondary and tertiary amines, and rotation of carboxylate groups, as well as torsion angle distribution and post-process rotatable bonds as default. The annealing parameters were used as default cutoff values of 3.0 Å for hydrogen bonds and 4.0 Å for van der Waals interactions. Hydrophobic fitting points were calculated to facilitate the correct starting orientation of the compound for docking by placing the hydrophobic atoms appropriately in the corresponding areas of the active site. When the top three solutions attained root-mean-square deviation (rmsd) values within 1.5 Å, docking was terminated. GOLD-Score, a scoring function within the software, is a dimensionless fitness value that takes into account the intra- and intermolecular hydrogen bonding interaction energy, van der Waals energy, and ligand torsion energy [42,43]. Protein-ligand interactions fingerprinting was generated using PyPLIF, a python program, which converts three-dimensional (3D) protein-ligand interactions into one-dimensional (1D) bitstrings [44]. There are seven types of possible interactions between ligand and every residue: (i) Apolar (van der Waals), (ii) aromatic face to face, (iii) aromatic edge to face, (iv) hydrogen bond (protein as hydrogen bond donor), (v) hydrogen bond (protein as hydrogen bond acceptor), (vi) electrostatic interaction (protein positively charged), and (vii) electrostatic interaction (protein negatively charged) [44]. Fingerprinting then clustered and plotted using matplotlib and seaborn (python packages for heat map, clustering, and plotting).

## Supplementary Material

Refer to Web version on PubMed Central for supplementary material.

## Acknowledgments

Supported by NIH awards R01CA253986 (to DL/NN) and R01GM101171 (to DL), DOD awards NF170044 (to DL/NN) and CA190267 (to DL), and Melanoma Research Alliance Team Science Award #396513.

## Data availability

Data will be made available on request.

## Abbreviations

| | |
|---|---|
| **SIRT5** | Sirtuin 5 |
| **SAR** | structure activity relationship |
| **LCMS** | liquid chromatography–mass spectrometry |
| **DMF** | *N,N*-dimethylformamide |
| **DCM** | dichloromethane |
| **EtOH** | ethanol |
| **DIPEA** | diisopropylethylamine |
| **TFA** | trifluoroacetic acid |

| | |
|---|---|
| **TEA** | triethylamine |

## References


[1]. Tanny JC, Dowd GJ, Huang J, Hilz H, Moazed D, An enzymatic activity in the yeast Sir2 protein that is essential for gene silencing, Cell 99 (1999) 735–745, 10.1016/S0092-8674(00)81671-2. [PubMed: 10619427]

[2]. Haigis MC, Mostoslavsky R, Haigis KM, Fahie K, Christodoulou DC, Murphy AJ, Valenzuela DM, Yancopoulos GD, Karow M, Blander G, Wolberger C, Prolla TA, Weindruch R, Alt FW, Guarente L, SIRT4 inhibits glutamate dehydrogenase and opposes the effects of calorie restriction in pancreatic β cells, Cell 126 (2006) 941–954, 10.1016/j.cell.2006.06.057. [PubMed: 16959573]

[3]. Meter MV, Mao Z, Gorbunova V, Seluanov A, Repairing split ends: SIRT6, mono-ADP ribosylation and DNA repair, Aging 3 (2011) 829–835, 10.18632/aging.100389. [PubMed: 21946623]

[4]. Frye RA, Phylogenetic classification of prokaryotic and eukaryotic Sir2-like proteins, Biochem. Biophys. Res. Commun 273 (2000) 793–798. 10.1006/bbrc.2000.3000. [PubMed: 10873683]

[5]. Giblin W, Skinner ME, Lombard DB, Sirtuins: guardians of mammalian healthspan, Trends Genet 30 (2014) 271–286, 10.1016/j.tig.2014.04.007. [PubMed: 24877878]

[6]. Kumar S, Lombard DB, Mitochondrial sirtuins and their relationships with metabolic disease and cancer, Antioxidants Redox Signal 22 (2015) 1060–1077, 10.1089/ars.2014.6213.

[7]. Du J, Zhou Y, Su X, Yu JJ, Khan S, Jiang H, Kim J, Woo J, Kim JH, Choi BH, He B, Chen W, Zhang S, Cerione RA, Auwerx J, Hao Q, Lin H, SIRT5 is a NAD-dependent protein lysine demalonylase and desuccinylase, Science 334 (2011) 806–809, 10.1126/science.1207861. [PubMed: 22076378]

[8]. Parihar P, Solanki I, Mansuri ML, Parihar MS, Mitochondrial sirtuins: emerging roles in metabolic regulations, energy homeostasis and diseases, Exp. Gerontol 61 (2015) 130–141, 10.1016/j.exger.2014.12.004. [PubMed: 25482473]

[9]. Nakagawa T, Lomb DJ, Haigis MC, Guarente L, SIRT5 deacetylates carbamoyl phosphate synthetase 1 and regulates the urea cycle, Cell 137 (2009) 560–570, 10.1016/j.cell.2009.02.026. [PubMed: 19410549]

[10]. Park J, Chen Y, Tishkoff DX, Peng C, Tan M, Dai L, Xie Z, Zhang Y, Zwaans BMM, Skinner ME, Lombard DB, Zhao Y, SIRT5-mediated lysine desuccinylation impacts diverse metabolic pathways, Mol. Cell 50 (2013) 919–930, 10.1016/j.molcel.2013.06.001. [PubMed: 23806337]

[11]. Nishida Y, Rardin MJ, Carrico C, He W, Sahu AK, Gut P, Najjar R, Fitch M, Hellerstein M, Gibson BW, Verdin E, SIRT5 regulates both cytosolic and mitochondrial protein malonylation with glycolysis as a major target, Mol. Cell 59 (2015) 321–332, 10.1016/j.molcel.2015.05.022. [PubMed: 26073543]

[12]. Polletta L, Vernucci E, Carnevale I, Arcangeli T, Rotili D, Palmerio S, Steegborn C, Nowak T, Schutkowski M, Pellegrini L, Sansone L, Villanova L, Runci A, Pucci B, Morgante E, Fini M, Mai A, Russo MA, Tafani M, SIRT5 regulation of ammonia-induced autophagy and mitophagy, Autophagy 11 (2015) 253–270, 10.1080/15548627.2015.1009778. [PubMed: 25700560]

[13]. Gertz M, Steegborn C, Function and regulation of the mitochondrial sirtuin isoform SIRT5 in mammalia, Biochim. Biophys. Acta 1804 (2010) 1658–1665, 10.1016/j.bbapap.2009.09.011. [PubMed: 19766741]

[14]. Lin Z-F, Xu H-B, Wang J-Y, Lin Q, Ruan Z, Liu F-B, Jin W, Huang H-H, Chen X, SIRT5 desuccinylates and activates SOD1 to eliminate ROS, Biochem. Biophys. Res. Commun 441 (2013) 191–195, 10.1016/j.bbrc.2013.10.033. [PubMed: 24140062]

[15]. Jing H, Lin H, Sirtuins in epigenetic regulation, Chem. Rev 115 (2015) 2350–2375, 10.1021/cr500457h. [PubMed: 25804908]

[16]. Bringman-Rodenbarger LR, Guo AH, Lyssiotis CA, Lombard DB, Emerging roles for SIRT5 in metabolism and cancer, Antioxidants Redox Signal 28 (2018) 677–690, 10.1089/ars.2017.7264.

[17]. Lu W, Zuo Y, Feng Y, Zhang M, SIRT5 facilitates cancer cell growth and drug resistance in non-small cell lung cancer, Tumor Biol 35 (2014) 10699–10705, 10.1007/s13277-014-2372-4.

[18]. Giblin W, Bringman-Rodenbarger L, Guo AH, Kumar S, Monovich AC, Mostafa AM, Skinner ME, Azar M, Mady AS, Chung CH, Kadambi N, Melong K-A, Lee H-J, Zhang L, Sajjakulnukit P, Trefely S, Varner EL, Iyer S, Wang M, Wilmott JS, Soyer HP, Sturm RA, Pritchard AL, Andea AA, Scolyer RA, Stark MS, Scott DA, Fullen DR, Bosenberg MW, Chandrasekaran S, Nikolovska-Coleska Z, Verhaegen ME, Snyder NW, Rivera MN, Osterman AL, Lyssiotis CA, Lombard DB, The deacylase SIRT5 supports melanoma viability by influencing chromatin dynamics, J. Clin. Invest 131 (2021), 138926, 10.1172/jci138926. [PubMed: 33945506]

[19]. Yang X, Wang Z, Li X, Liu B, Liu M, Liu L, Chen S, Ren M, Wang Y, Yu M, Wang B, Zou J, Zhu W-G, Yin Y, Gu W, Luo J, SHMT2 desuccinylation by SIRT5 drives cancer cell proliferation, Cancer Res 78 (2018) 372–386, 10.1158/0008-5472.CAN-17-1912. [PubMed: 29180469]

[20]. Wang Y-Q, Wang H-L, Xu J, Tan J, Fu L-N, Wang J-L, Zou T-H, Sun D-F, Gao Q-Y, Chen Y-X, Fang J-Y, Sirtuin5 contributes to colorectal carcinogenesis by enhancing glutaminolysis in a deglutarylation-dependent manner, Nat. Commun 9 (2018) 545, 10.1038/s41467-018-02951-4. [PubMed: 29416026]

[21]. Shi L, Yan H, An S, Shen M, Jia W, Zhang R, Zhao L, Huang G, Liu J, SIRT5-mediated deacetylation of LDHB promotes autophagy and tumorigenesis in colorectal cancer, Mol. Oncol 13 (2019) 358–375, 10.1002/1878-0261.12408. [PubMed: 30443978]

[22]. Bai L, Yang Z-X, Ma P-F, Liu J-S, Wang D-S, Yu H-C, Overexpression of SLC25A51 promotes hepatocellular carcinoma progression by driving aerobic glycolysis through activation of SIRT5, Free Radic. Biol. Med 182 (2022) 11–22, 10.1016/j.freeradbiomed.2022.02.014. [PubMed: 35182732]

[23]. He B, Du J, Lin H, Thiosuccinyl peptides as SIRT5-specific inhibitors, J. Am. Chem. Soc 134 (2012) 1922–1925, 10.1021/ja2090417. [PubMed: 22263694]

[24]. Roessler C, Nowak T, Pannek M, Gertz M, Nguyen GTT, Scharfe M, Born I, Sippl W, Steegborn C, Schutkowski M, Chemical probing of the human sirtuin 5 active site reveals its substrate acyl specificity and peptide-based inhibitors, Angew. Chem., Int. Ed 53 (2014) 10728–10732, 10.1002/anie.201402679.

[25]. Maurer B, Rumpf T, Scharfe M, Stolfa DA, Schmitt ML, He W, Verdin E, Sippl W, Jung M, Inhibitors of the $NAD^+$-dependent protein desuccinylase and demalonylase SIRT5, ACS Med. Chem. Lett 3 (2012) 1050–1053, 10.1021/ml3002709. [PubMed: 24900427]

[26]. Suenkel B, Fischer F, Steegborn C, Inhibition of the human deacylase Sirtuin 5 by the indole GW5074, Bioorg. Med. Chem. Lett 23 (2013) 143–146, 10.1016/j.bmcl.2012.10.136. [PubMed: 23195732]

[27]. Yang L-L, He Y-Y, Chen Q-L, Qian S, Wang Z-Y, Design and synthesis of new 9-substituted norharmane derivatives as potential SIRT5 inhibitors, J. Heterocycl. Chem 54 (2017) 1457–1466, 10.1002/jhet.2732.

[28]. Liu S, Ji S, Yu Z-J, Wang H-L, Cheng X, Li W-J, Jing L, Yu Y, Chen Q, Yang L-L, Li G-B, Wu Y, Structure-based discovery of new selective small-molecule sirtuin 5 inhibitors, Chem. Biol. Drug Des 91 (2018) 257–268, 10.1111/cbdd.13077. [PubMed: 28756638]

[29]. Yang L, Ma X, He Y, Yuan C, Chen Q, Li G, Chen X, Sirtuin 5: a review of structure, known inhibitors and clues for developing new inhibitors, Sci. China, Life Sci 60 (2017) 249–256, 10.1007/s11427-016-0060-7.

[30]. Rajabi N, Auth M, Troelsen KR, Pannek M, Bhatt DP, Fontenas M, Hirschey MD, Steegborn C, Madsen AS, Olsen CA, Mechanism-based inhibitors of the human sirtuin 5 deacylase: structure-activity relationship, biostructural, and kinetic insight, Angew. Chem., Int. Ed 56 (2017) 14836–14841, 10.1002/anie.201709050.

[31]. Kalbas D, Liebscher S, Nowak T, Meleshin M, Pannek M, Popp C, Alhalabi Z, Bordusa F, Sippl W, Steegborn C, Schutkowski M, Potent and selective inhibitors of human sirtuin 5, J. Med. Chem 61 (2018) 2460–2471, 10.1021/acs.jmedchem.7b01648. [PubMed: 29494161]

[32]. Glas C, Dietschreit JCB, Wossner N, Urban L, Ghazy E, Sippl W, Jung M, Ochsenfeld C, Bracher F, Identification of the subtype-selective Sirt5 inhibitor balsalazide through systematic SAR analysis and rationalization via theoretical investigations, Eur. J. Med. Chem 206 (2020), 112676, 10.1016/j.ejmech.2020.112676. [PubMed: 32858418]

[33]. Yang F, Su H, Deng J, Mou L, Wang H, Li R, Dai Q-Q, Yan Y-H, Qian S, Wang Z, Li G-B, Yang L, Discovery of new human Sirtuin 5 inhibitors by mimicking glutaryl-lysine substrates, Eur. J. Med. Chem 225 (2021), 113803, 10.1016/j.ejmech.2021.113803. [PubMed: 34461505]

[34]. Jiang Y, Zheng W, Cyclic tripeptide-based potent and selective human SIRT5 inhibitors, Med. Chem 16 (2020) 358–367, 10.2174/1573406415666190603101937. [PubMed: 31161996]

[35]. Madsen AS, Olsen CA, Substrates for efficient fluorometric screening employing the NAD-dependent sirtuin 5 lysine deacylase (KDAC) enzyme, J. Med. Chem 55 (2012) 5582–5590, 10.1021/jm300526r. [PubMed: 22583019]

[36]. Wang H-L, Liu S, Yu Z-J, Wu C, Cheng L, Wang Y, Chen K, Zhou S, Chen Q, Yu Y, Li G-B, Interactions between sirtuins and fluorogenic small-molecule substrates offer insights into inhibitor design, RSC Adv 7 (2017) 36214–36222, 10.1039/C7RA05824A.

[37]. Schuetz A, Min J, Antoshenko T, Wang C-L, Allali-Hassani A, Dong A, Loppnau P, Vedadi M, Bochkarev A, Sternglanz R, Plotnikov AN, Structural basis of inhibition of the human $NAD^+$-dependent deacetylase SIRT5 by suramin, Structure 15 (2007) 377–389, 10.1016/j.str.2007.02.002. [PubMed: 17355872]

[38]. Zang W, Hao Y, Wang Z, Zheng W, Novel thiourea-based sirtuin inhibitory warheads, Bioorg. Med. Chem. Lett 25 (2015) 3319–3324, 10.1016/j.bmcl.2015.05.058. [PubMed: 26081291]

[39]. Hirsch BM, Hao Y, Li X, Wesdemiotis C, Wang Z, Zheng W, A mechanism-based potent sirtuin inhibitor containing Nε-thiocarbamoyl-lysine (TuAcK), Bioorg. Med. Chem. Lett 21 (2011), 10.1016/j.bmcl.2011.06.069, 4753–4747. [PubMed: 21752644]

[40]. GOLD Software Package, Version 5.3, Cambridge Crystallographic Data Centre, Cambridge, U.K., https://www.ccdc.cam.ac.uk.

[41]. OMEGA 3.1.2.2: OpenEye Scientific Software, Santa Fe, NM http://www.eyesopen.com.

[42]. Jones G, Willett P, Docking small-molecule ligands into active sites, Curr. Opin. Biotechnol 6 (1995) 652–656, 10.1016/0958-1669(95)80107-3. [PubMed: 8527835]

[43]. Jones G, Willett P, Glen RC, Leach AR, Taylor R, Development and validation of a genetic algorithm for flexible docking, J. Mol. Biol 267 (1997) 727–748, 10.1006/jmbi.1996.0897. [PubMed: 9126849]

[44]. Radifar M, Yuniarti N, Istyastono EP, PyPLIF: python-based protein-ligand interaction fingerprinting, Bioformation 9 (2013) 325–328, 10.6026/97320630009325.

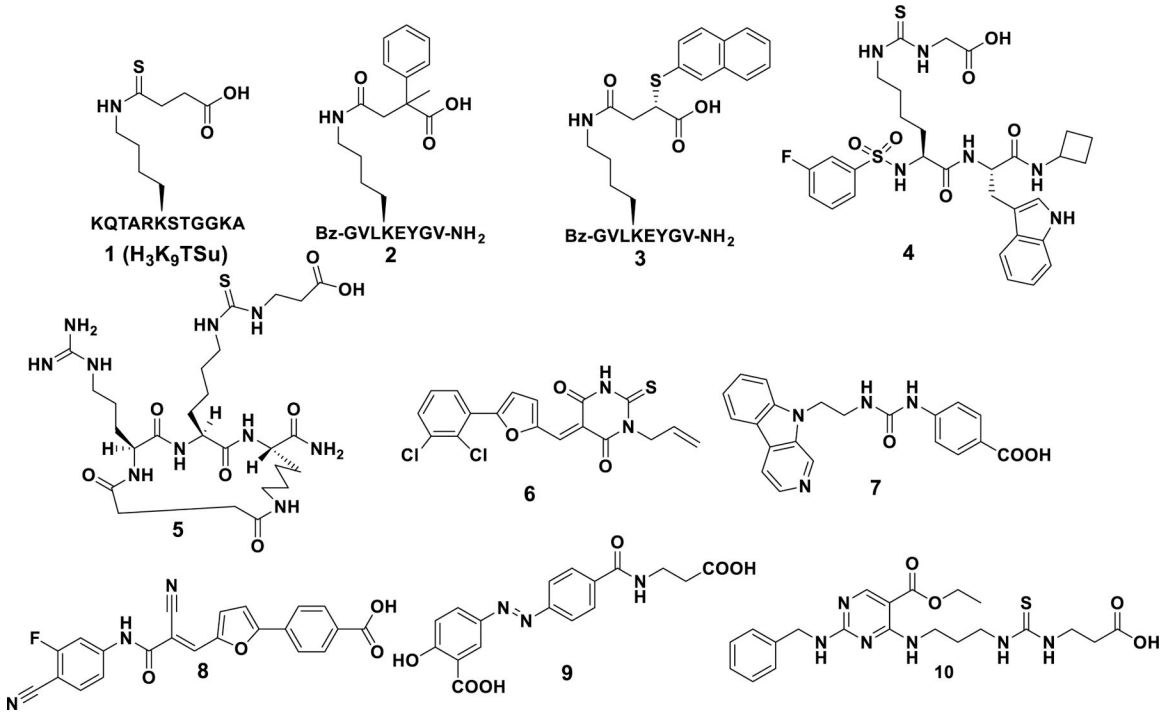


**Fig. 1.**
Reported SIRT5 inhibitors.

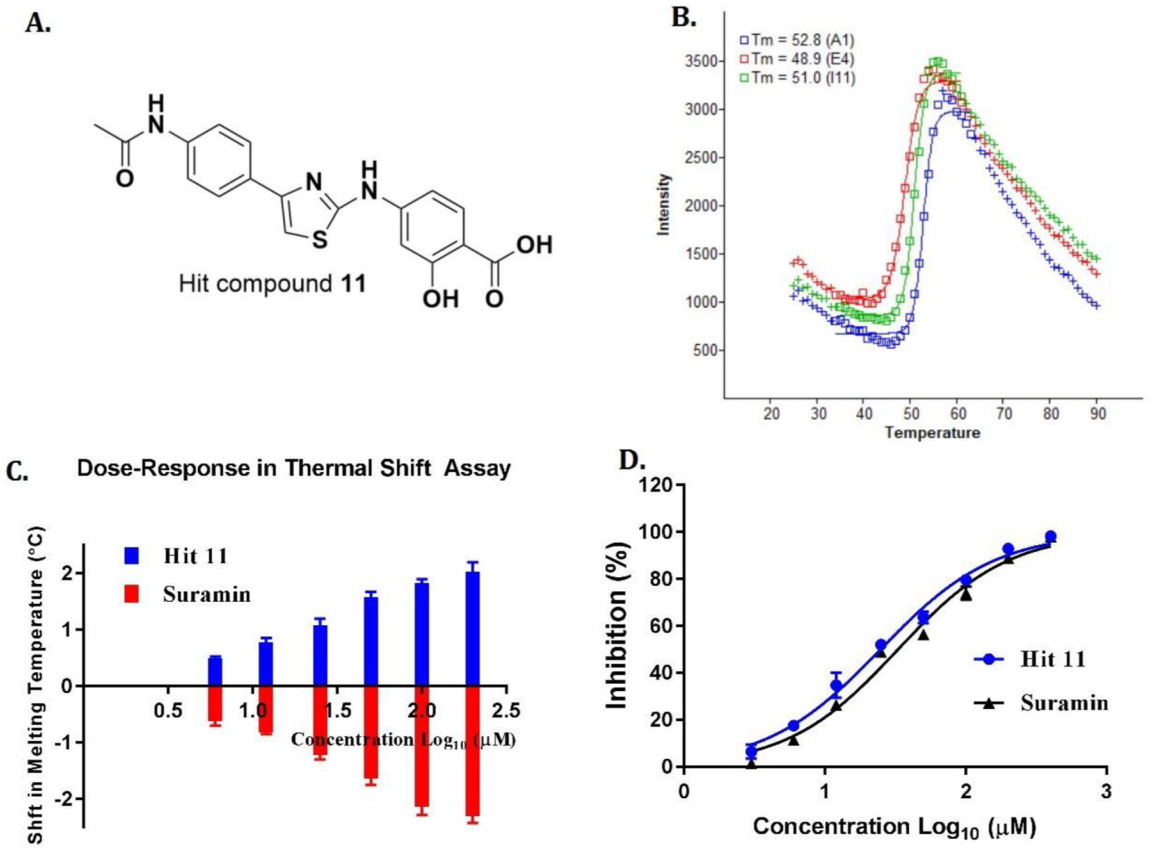


**Fig. 2.**

(A) Structure of hit compound **11**. (B) Thermal melting curve of **11** at 100 μM versus reference (DMSO) control and a positive control (suramin). A1 (blue curve): sample well contains **11**, wild type SIRT5, dye, and buffer; I11 (green curve): reference (DMSO) control well contains DMSO, wild type SIRT5, dye, and buffer; E4 (red curve): positive control well contains suramin, wild type SIRT5, dye, and buffer. The melting curve is presented as fluorescence intensity versus temperature. (C) Concentration-dependent stabilization of SIRT5 by **11**. The ΔTm was measured as above using SIRT5 and compound **11** (6–200 μM). The curve represents an exponential fit to the ΔTm values plotted against the compound concentration. (D) Concentration-dependent inhibition of SIRT5 by hit **11**. All measurements were done in quadruplicates. Reported SIRT5 inhibitor suramin was used as a positive control.

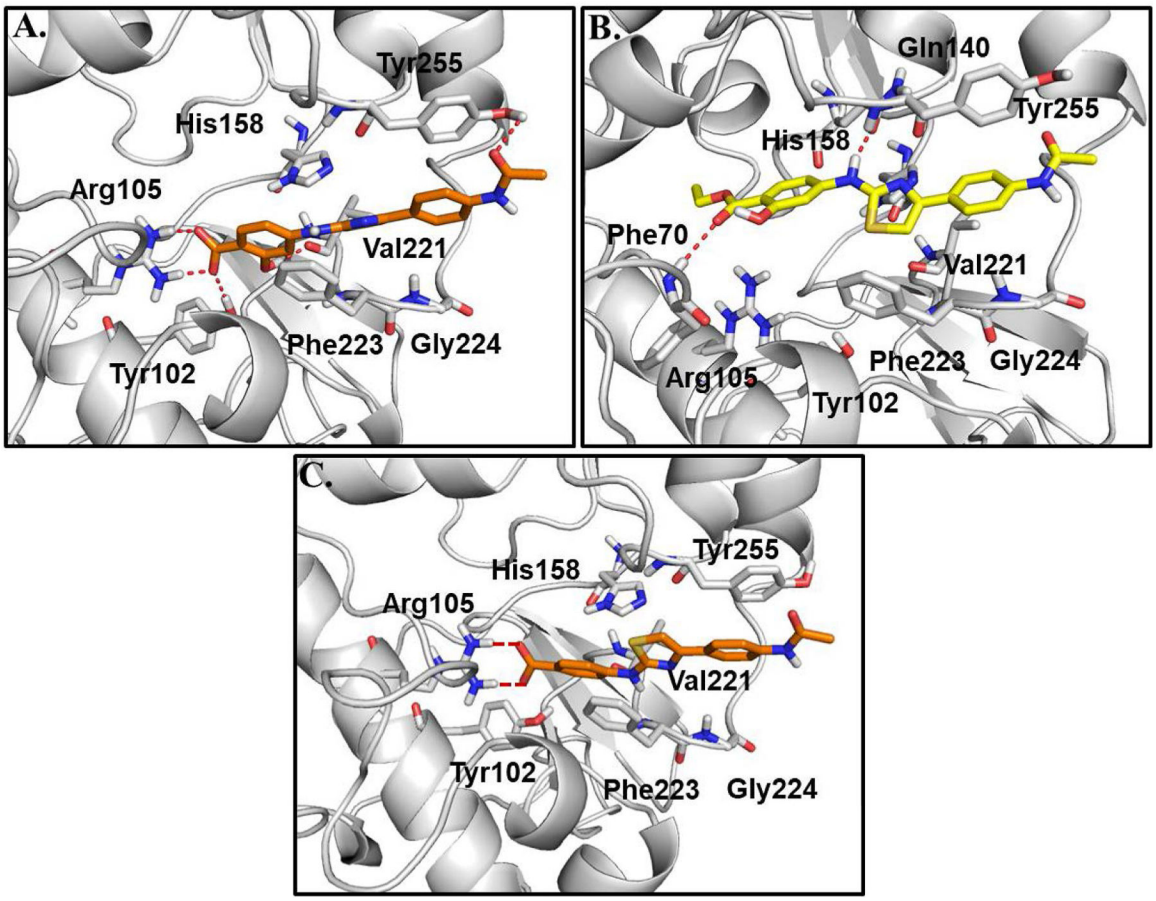


**Fig. 3.**

(A) The predicted binding modes of compound **11** with SIRT5. (B & C) The predicted binding modes of inactive compounds **12** and **13**, respectively with SIRT5.

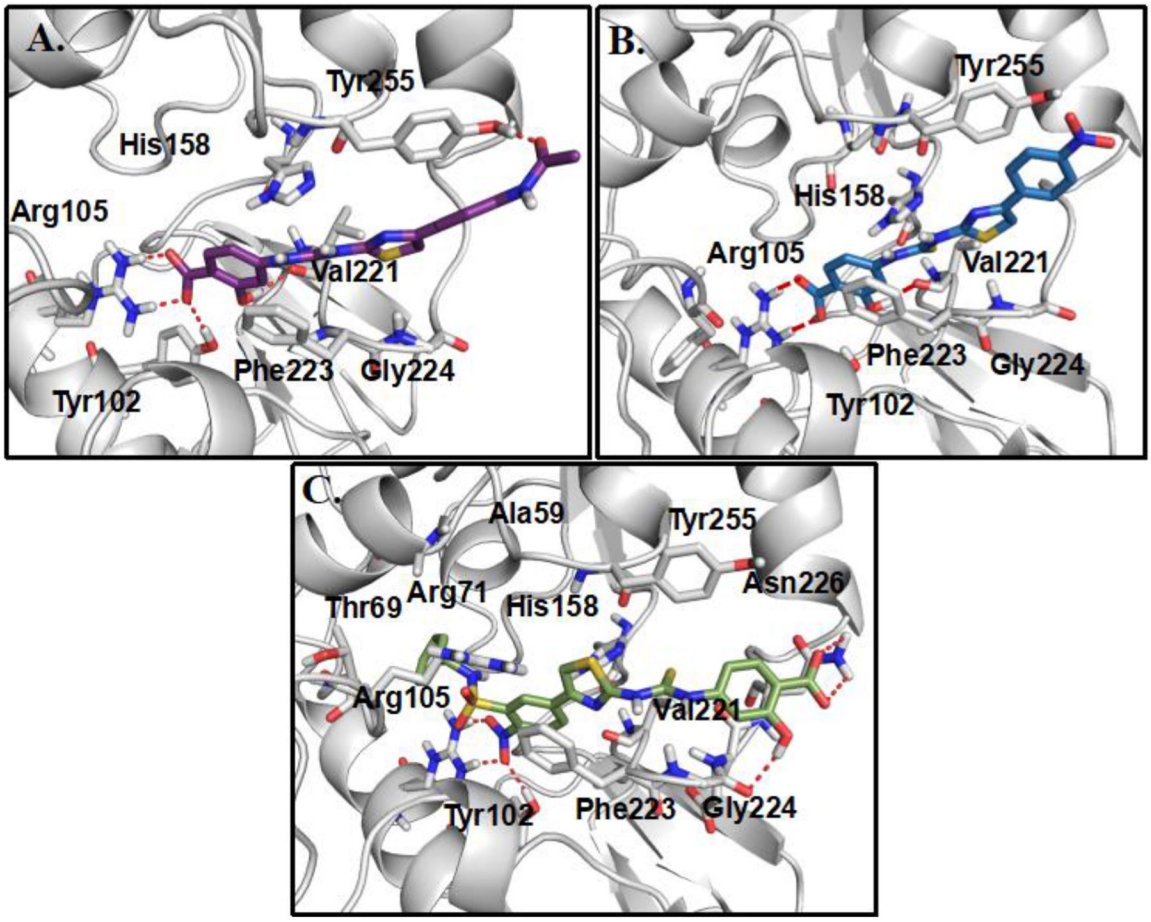


**Fig. 4.**

(A) The predicted binding modes of compounds **14** (A), **30** (B) and **43** (C) with SIRT5, respectively.

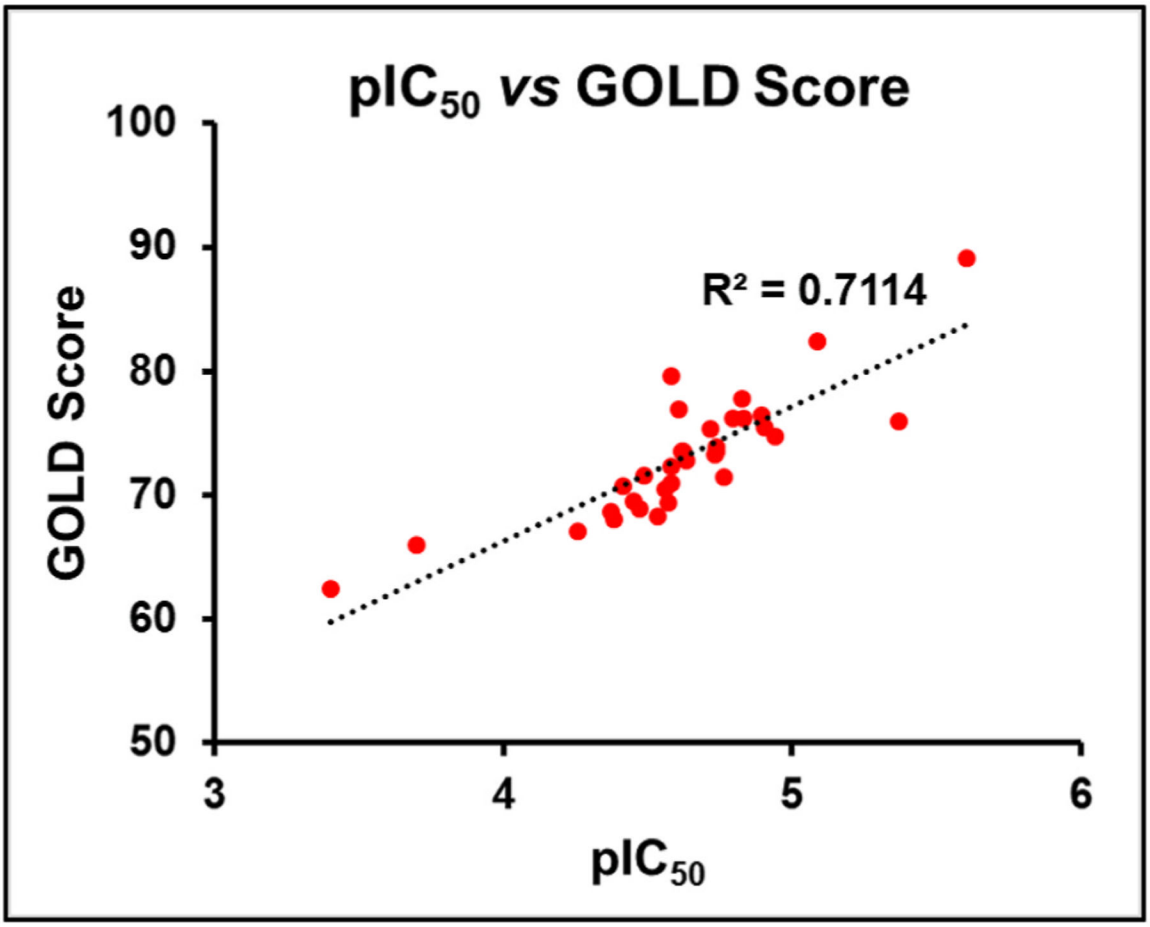


**Fig. 5.**
Docking score (GOLD score) vs $pIC_{50}$ values.

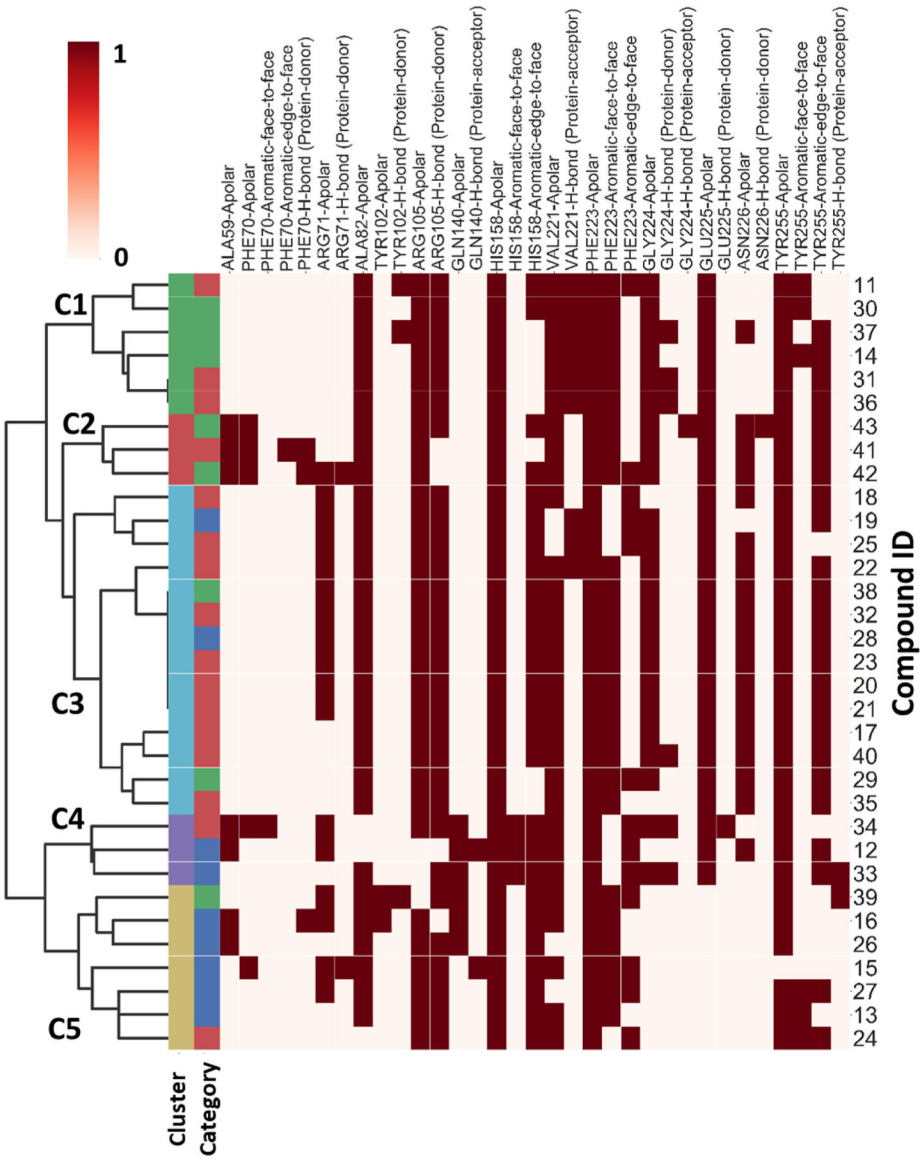


**Fig. 6.**

Protein-ligand interactions fingerprinting of compounds **11**–**43** with the key residues of SIRT5 protein. At the top, the x-axis represents key residues with seven different types of interactions. If the interactions are present, then the cells are in red, otherwise no color. On the left, a dendrogram is drawn to show the relationship between different clusters (C1–C5). The first column at the left represents color-coded clusters of fingerprints. Second column from the left represents category of compounds based on enzymatic activity; actives ($pIC_{50}$ > 4.8), moderately actives (4.8 ≤ $pIC_{50}$ ≥ 4.5) and inactives ($pIC_{50}$ < 4.5).

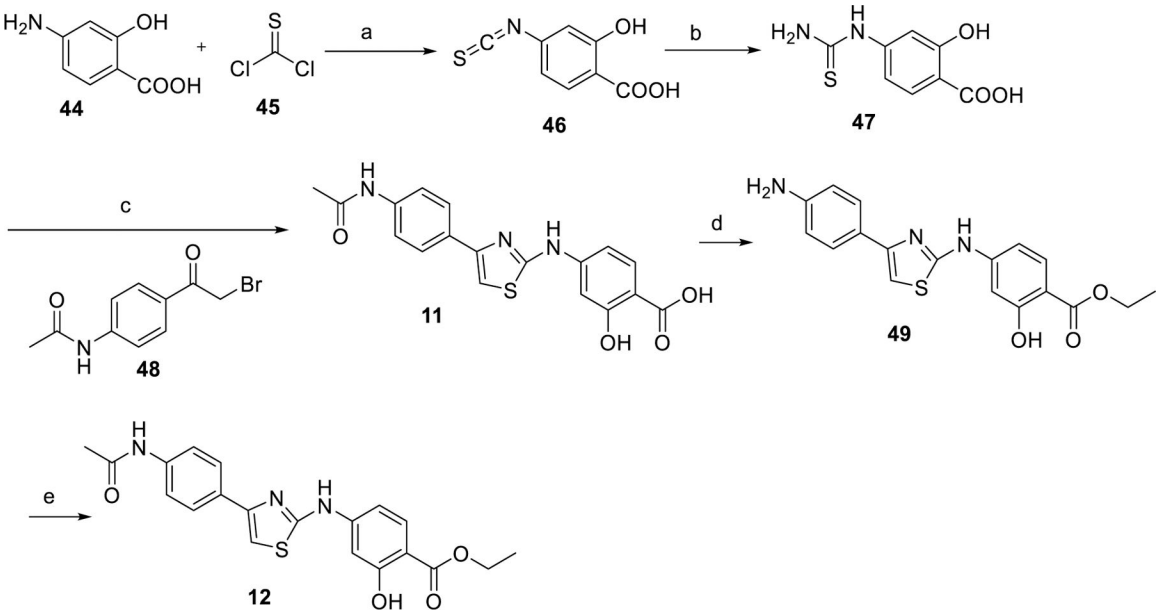


**Scheme 1.**

Synthesis of hit compound 11 and 12[a]

[a]Reaction conditions: (a) HCl, $H_2O$, rt; (b) aqueous ammonia, rt; (c) *N*-(4-(2-bromoacetyl)phenyl)acetamide, EtOH, reflux; (d) $H_2SO_4$, EtOH, reflux; (e) acetylchloride, DMF, 0 °C to rt.

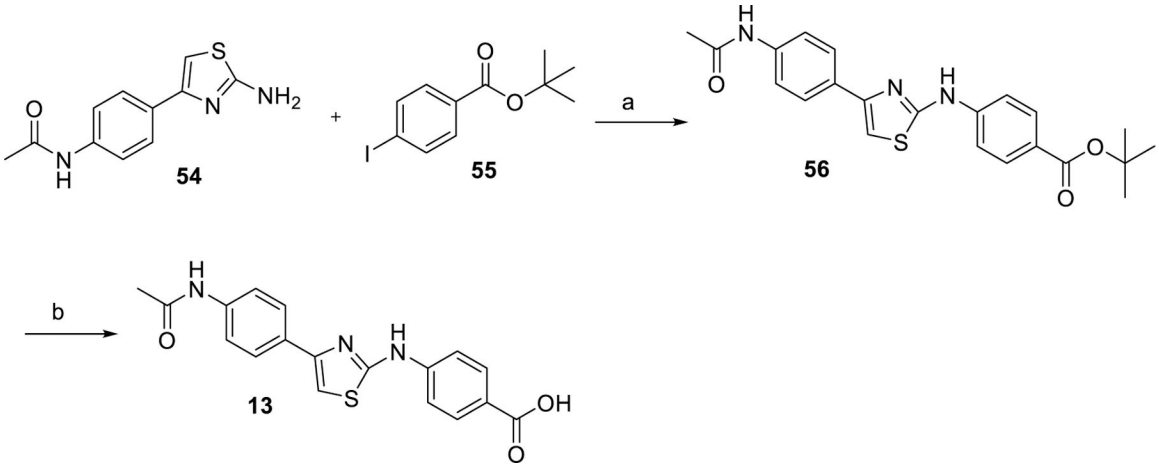


**Scheme 2.**

Synthesis of compound 13[a]

[a]Reagents and conditions: (a) $Pd(OAc)_2$, BINAP, $Cs_2CO_3$, DMF, 100 °C; (b) TFA, DCM, rt.

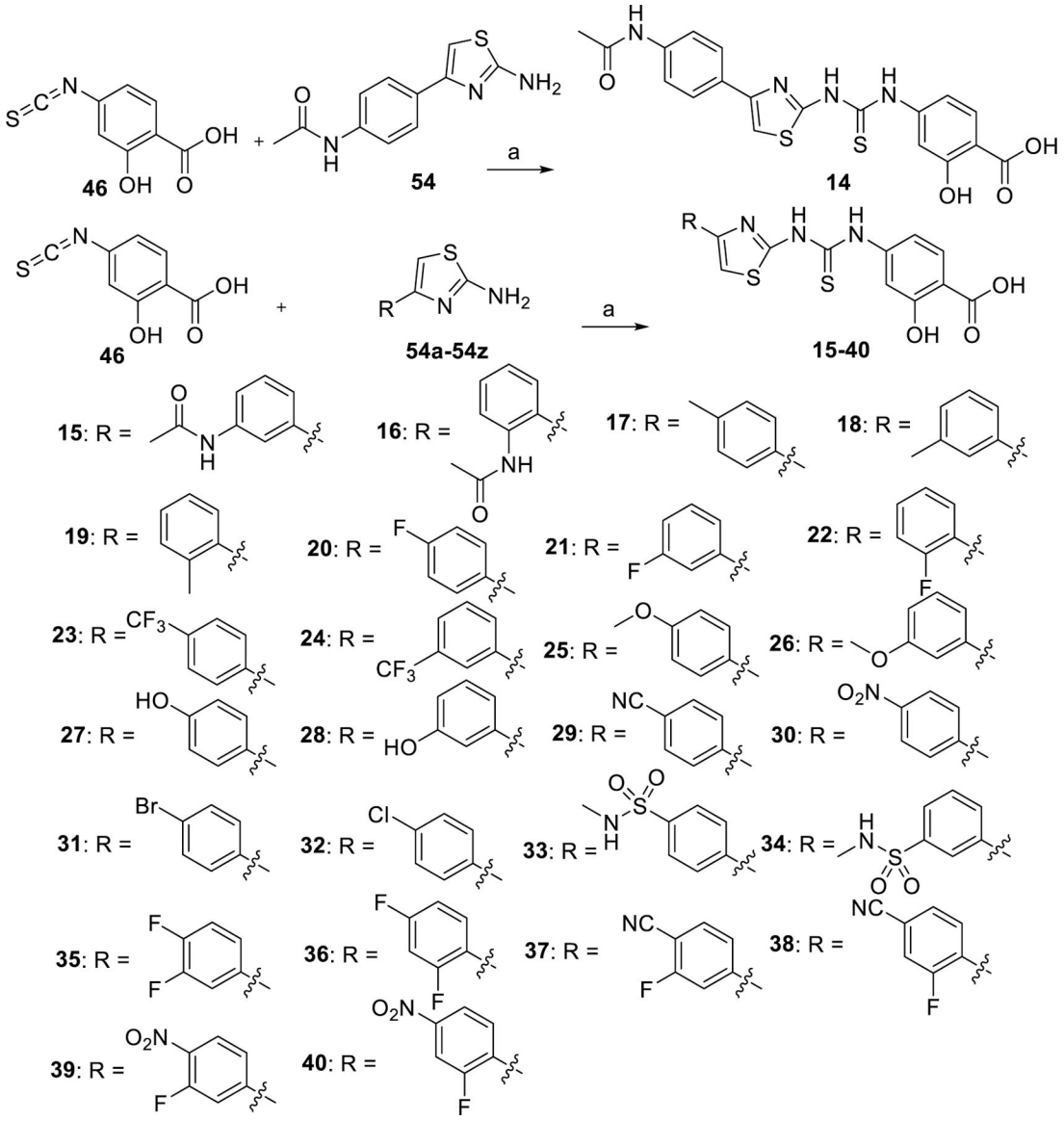


**Scheme 3.**

Synthesis of compound 14–40[a]

[a]Reaction conditions: (a) pyridine, 60 °C.

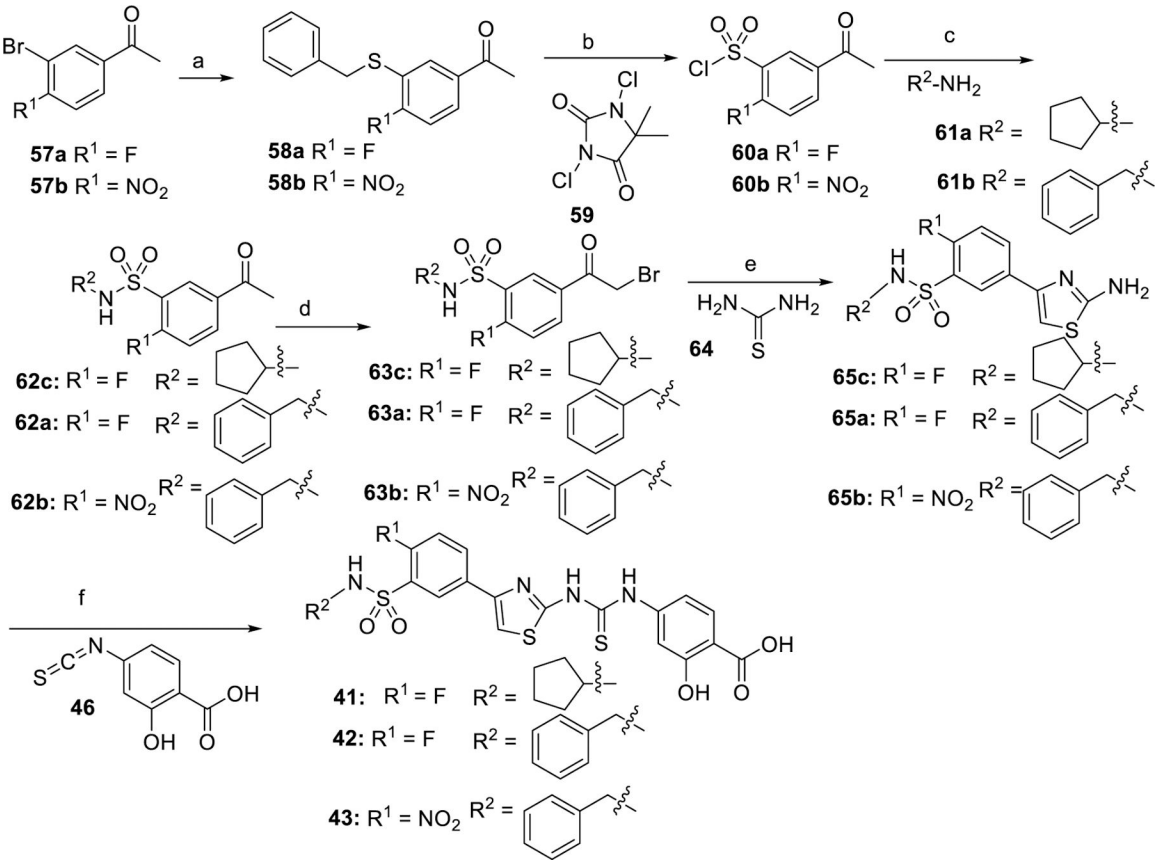


**Scheme 4.**

Synthesis of compound 41–43[a]

[a]Reaction conditions: (a) DIPEA, 1,4 dioxane, $Pd_2(dba)_3$, Xantphos, benzylthiol, reflux; (b) $CH_3CN$, $H_2O$, AcOH, 0 °C; (c) TEA, DCM, rt; (d) $Bu_4NBr_3$, $CH_3CN$, 60 °C; (e) EtOH, reflux; (f) pyridine, 60 °C.

**Table 1**

The SIRT5 inhibitory activities of analogues 11–13[a].

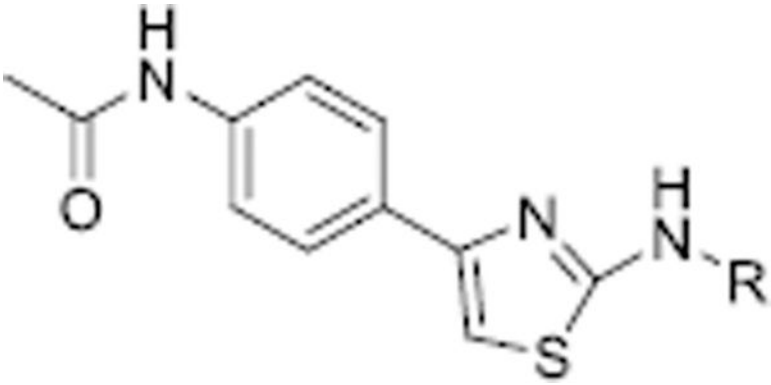


| Cpd. | R | SIRT5 $IC_{50}$ (μM) | [b] $\Delta$Tm (°C) | [c] cLogP | [d] LE |
|---|---|---|---|---|---|
| 11 | 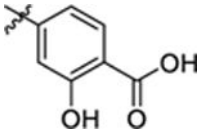 | 26.4 ± 0.8 | 1.8 ± 0.1 | 4.04 | 0.25 |
| 12 | 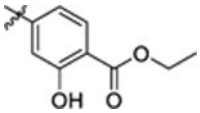 | >400 | 0.12 ± 0.08 | 4.64 | – |
| 13 | 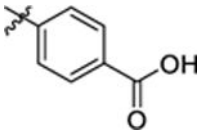 | 200.6 ± 8.9 | 0.53 ± 0.17 | 3.97 | 0.21 |

[a] Suramin was used as a positive control with an $IC_{50}$ of 28.4 ± 2.5 μM.

[b] The ΔTm values were calculated from the thermal shift assay at a compound concentration of 100 μM.

[c] cLogP values were calculated using ChemDraw Ultra 12.0.

[d] Calculated LE = 1.4 $pIC_{50}$ (M)/N, where N is the number of non-hydrogen atom.

**Table 2**

The SIRT5 inhibitory activities of analogues 14–43[a].

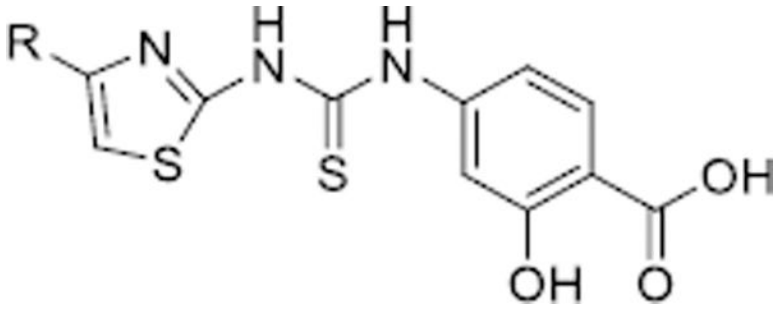


| Cpd. | R | SIRT5 $IC_{50}$ (μM) | [b] $\Delta Tm$ (°C) | [c] cLogP | [d] LE |
|---|---|---|---|---|---|
| 14 | 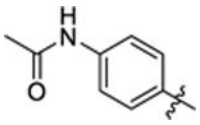 | 12.4 ± 0.6 | 2.5 ± 0.2 | 2.74 | 0.24 |
| 15 | 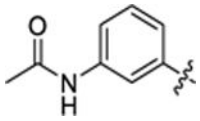 | 35.6 ± 1.3 | 1.5 ± 0.2 | 2.74 | 0.21 |
| 16 | 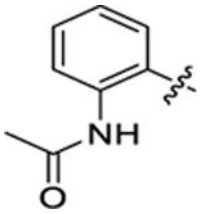 | 55.6 ± 5.5 | 0.9 ± 0.1 | 1.71 | 0.20 |
| 17 | 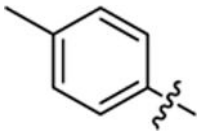 | 23.4 ± 0.9 | 1.4 ± 0.1 | 4.04 | 0.25 |
| 18 | 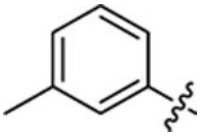 | 27.7 ± 1.0 | 1.2 ± 0.2 | 4.04 | 0.25 |
| 19 | 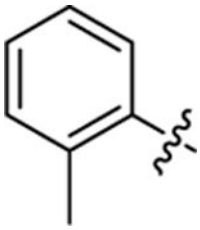 | 34.0 ± 2.2 | 1.1 ± 0.2 | 3.74 | 0.24 |

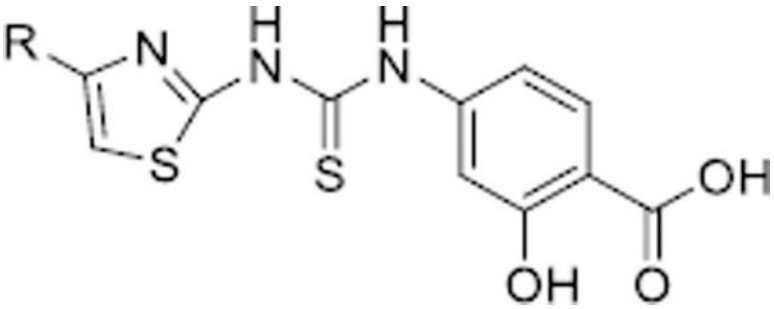


| Cpd. | R | SIRT5 $IC_{50}$ (μM) | $^{b}\Delta Tm$ (°C) | $^{c}cLogP$ | $^{d}LE$ |
|---|---|---|---|---|---|
| 20 | 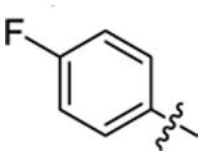 | 17.3 ± 0.3 | 1.3 ± 0.2 | 3.69 | 0.26 |
| 21 | 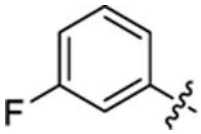 | 18.3 ± 1.0 | 1.22 ± 0.1 | 3.69 | 0.26 |
| 22 | 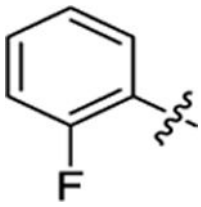 | 26.2 ± 2.5 | 1.0 ± 0.2 | 3.69 | 0.25 |
| 23 | 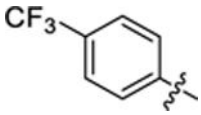 | 24.3 ± 2.5 | 1.2 ± 0.1 | 4.43 | 0.22 |
| 24 | 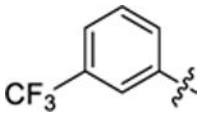 | 26.8 ± 1.4 | 1.1 ± 0.1 | 4.43 | 0.22 |
| 25 | 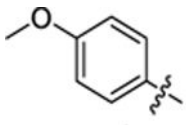 | 29.2 ± 2.9 | 0.9 ± 0.2 | 3.56 | 0.24 |
| 26 | 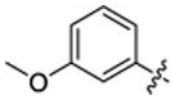 | 41.6 ± 3.8 | 0.9 ± 0.1 | 3.56 | 0.23 |

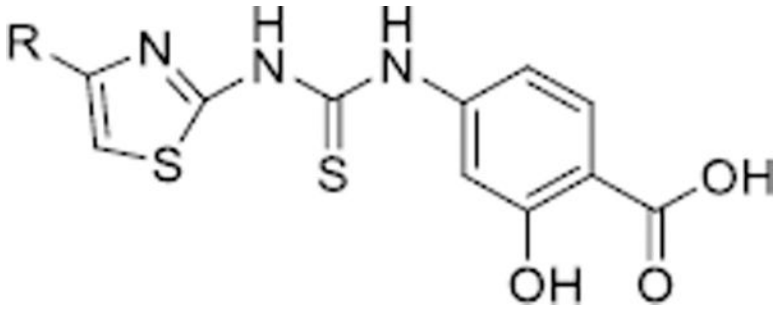

| Cpd. | R | SIRT5 $IC_{50}$ (μM) | $^{b}\Delta Tm$ (°C) | $^{c}cLogP$ | $^{d}LE$ |
|---|---|---|---|---|---|
| 27 | 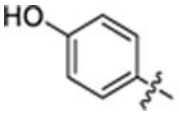 | 42.5 ± 3.8 | 0.8 ± 0.1 | 3.08 | 0.24 |
| 28 | 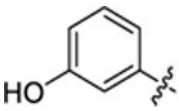 | 32.8 ± 3.9 | 0.72 ± 0.1 | 3.08 | 0.24 |
| 29 | 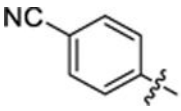 | 11.4 ± 0.5 | 2.1 ± 0.3 | 2.98 | 0.26 |
| 30 | 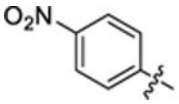 | 4.3 ± 0.3 | 1.8 ± 0.2 | 3.29 | 0.27 |
| 31 | 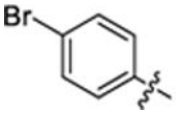 | 18.6 ± 0.2 | 1.2 ± 0.1 | 4.40 | 0.25 |
| 32 | 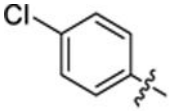 | 18.4 ± 0.3 | 1.1 ± 0.1 | 4.26 | 0.25 |
| 33 | 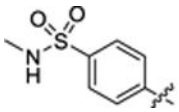 | 38.8 ± 3.1 | 0.9 ± 0.1 | 2.53 | 0.21 |
| 34 | 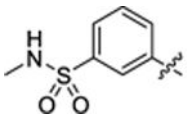 | 26.1 ± 1.9 | 0.8 ± 0.2 | 2.53 | 0.21 |

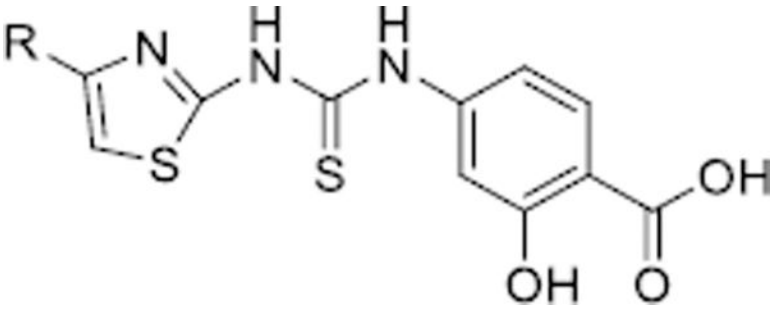


| Cpd. | R | SIRT5 $IC_{50}$ (μM) | $^{b}\Delta Tm$ (°C) | $^{c}cLogP$ | $^{d}LE$ |
|---|---|---|---|---|---|
| 35 | 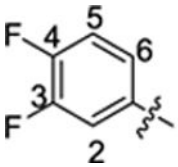 | 16.1 ± 0.7 | 1.8 ± 0.1 | 3.76 | 0.25 |
| 36 | 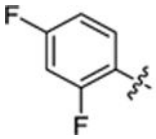 | 19.3 ± 0.9 | 1.9 ± 0.2 | 3.83 | 0.24 |
| 37 | 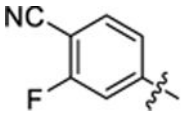 | 12.8 ± 0.5 | 1.8 ± 0.1 | 3.13 | 0.24 |
| 38 | 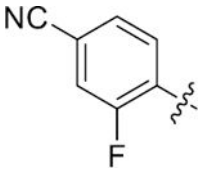 | 14.8 ± 0.8 | 1.9 ± 0.1 | 3.13 | 0.24 |
| 39 | 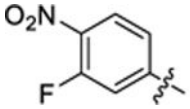 | 14.9 ± 1.3 | 1.8 ± 0.1 | 3.14 | 0.23 |
| 40 | 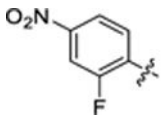 | 23.8 ± 2.7 | 1.6 ± 0.1 | 3.44 | 0.22 |
| 41 | 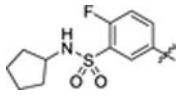 | 24.9 ± 0.5 | 1.3 ± 0.2 | 4.32 | 0.18 |
| 42 | 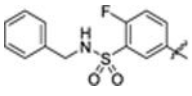 | 8.2 ± 1.3 | 1.9 ± 0.1 | 4.61 | 0.19 |

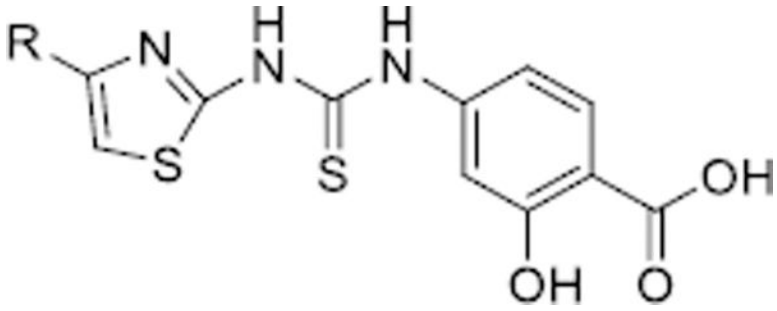


| Cpd. | R | SIRT5 $IC_{50}$ (μM) | [b] ΔTm (°C) | [c] cLogP | [d] LE |
|---|---|---|---|---|---|
| 43 | 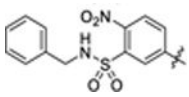 | 2.5 ± 0.2 | 1.8 ± 0.1 | 4.38 | 0.20 |

[a] Suramin was used as a positive control with an $IC_{50}$ of 28.4 ± 2.5 μM.

[b] The ΔTm values were calculated from the thermal shift assay at a compound concentration of 100 μM.

[c] cLogP values were calculated using ChemDraw Ultra 12.0.

[d] Calculated LE = 1.4 $pIC_{50}$ (M)/N, where N is the number of nonhydrogen atom.